Journal of Rock Mechanics and Geotechnical Engineering 8 (2016) 577–595

Contents lists available at ScienceDirect

Journal of Rock Mechanics and Geotechnical Engineering

journal homepage: www.rockgeotech.org

Full length article

Reservoir-induced landslides and risk control in Three Gorges Project on Yangtze River, China

Yueping Yin [a], Bolin Huang [b,*], Wenpei Wang [a], Yunjie Wei [a], Xiaohan Ma [c], Fei Ma [d], Changjun Zhao [e]

[a] China Institute of Geo-Environment Monitoring, China Geological Survey, Beijing, 100081, China
[b] Wuhan Center of China Geological Survey, Wuhan, 430205, China
[c] Department of Land and Resources of Hubei Province, Wuhan, 430071, China
[d] Department of Land and Resources of Chongqing, Chongqing, 400015, China
[e] Changjiang Institute of Survey, Planning, Design and Research Co., Ltd., Wuhan, 430010, China

ARTICLE INFO

Article history:
Received 2 October 2015
Received in revised form
31 July 2016
Accepted 3 August 2016
Available online 29 August 2016

Keywords:
Three Gorges Reservoir (TGR)
Reservoir-induced landslide
Reactivation mechanism
Impulsive wave generated by landslide
Water level variation
Risk control

ABSTRACT

The Three Gorges region in China was basically a geohazard-prone area prior to construction of the Three Gorges Reservoir (TGR). After construction of the TGR, the water level was raised from 70 m to 175 m above sea level (ASL), and annual reservoir regulation has caused a 30-m water level difference after impoundment of the TGR since September 2008. This paper first presents the spatiotemporal distribution of landslides in six periods of 175 m ASL trial impoundments from 2008 to 2014. The results show that the number of landslides sharply decreased from 273 at the initial stage to less than ten at the second stage of impoundment. Based on this, the reservoir-induced landslides in the TGR region can be roughly classified into five failure patterns, i.e. accumulation landslide, dip-slope landslide, reversed bedding landslide, rockfall, and karst breccia landslide. The accumulation landslides and dip-slope landslides account for more than 90%. Taking the Shuping accumulation landslide (a sliding mass volume of 20.7 $\times$ 10^6 m^3) in Zigui County and the Outang dip-slope landslide (a sliding mass volume of about 90 $\times$ 10^6 m^3) in Fengjie County as two typical cases, the mechanisms of reactivation of the two landslides are analyzed. The monitoring data and factor of safety (FOS) calculation show that the accumulation landslide is dominated by water level variation in the reservoir as most part of the mass body is under 175 m ASL, and the dip-slope landslide is controlled by the coupling effect of reservoir water level variation and precipitation as an extensive recharge area of rainfall from the rear and the front mass is below 175 m ASL. The characteristics of landslide-induced impulsive wave hazards after and before reservoir impoundment are studied, and the probability of occurrence of a landslide-induced impulsive wave hazard has increased in the reservoir region. Simulation results of the Ganjingzi landslide in Wushan County indicate the strong relationship between landslide-induced surge and water variation with high potential risk to shipping and residential areas. Regarding reservoir regulation in TGR when using a single index, i.e. 1-d water level variation, water resources are not well utilized, and there is also potential risk of disasters since 2008. In addition, various indices such as 1-d, 5-d, and 10-d water level variations are proposed for reservoir regulation. Finally, taking reservoir-induced landslides in June 2015 for example, the feasibility of the optimizing indices of water level variations is verified.

1. Introduction

Located in the transition zone between the second and third steps of China's topography with complicated geological environments, the Three Gorges region is a landslide-prone area (Liu et al., 1992). In July 1982, more than 81,000 landslides were reported in Wanzhou, Yunyang, Fengjie, Wushan, and other areas (Li, 1984; Chengdu College of Geology, 1986). In June 1985, the ancient

* Corresponding author.
E-mail address: bolinhuang@aliyun.com (B. Huang).
Peer review under responsibility of Institute of Rock and Soil Mechanics, Chinese Academy of Sciences.

http://dx.doi.org/10.1016/j.jrmge.2016.08.001

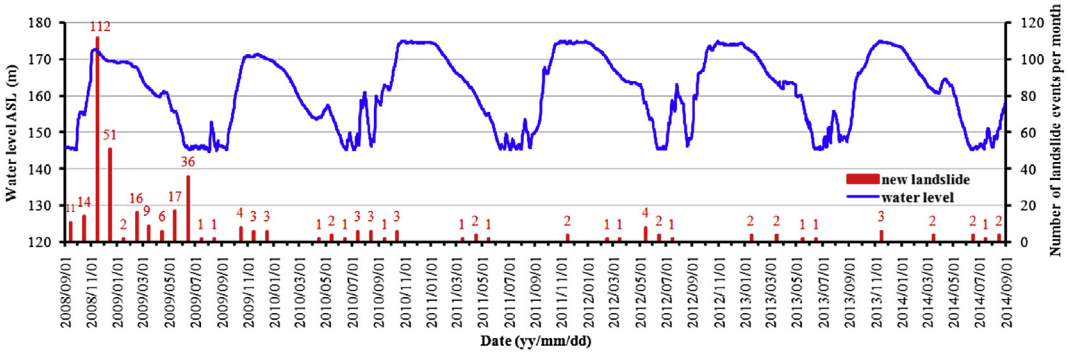

Fig. 1. Hydrograph of six periods occurred in 175 m ASL trial impoundment and water level drawdown.

town Xintan was destroyed by the Xintan landslide with a mass volume up to 30 × 10^6 m^3 on the left bank of the Yangtze River. Meanwhile, the toe mass of about 2 × 10^6 m^3 rushed into the river and generated waves of 54 m in height. The Yangtze River was blocked for 12 d (Chen et al., 1985; Liu, 1987). The construction of the Three Gorges Reservoir (TGR) was launched in 1994 with total reservoir water storage up to 39.3 × 10^9 m^3. The distance from the dam site to the reservoir rear is 663 km, with a total riparian line length of 5972 km. Two cities, 11 counties and 116 towns in the reservoir region could be drowned by reservoir impoundment and thus should be relocated, involving 1.2 million people. However, relocation to the upward terrace of the slope on the original spot is subjected to the threats of landslides and other geological hazards. Therefore, comprehensive prevention of geological hazards has been carried out since 2001. In this regard, more than 400 landslides, 300 unstable reservoir banks, and 2900 high cutting slopes have been reinforced, which has significantly enhanced the overall geological stability in relocation towns (Yin, 2005).

In September 2008, a trial impoundment of 175 m above sea level (ASL) commenced in TGR. The water level increased by about 100 m from the original water level of about 75 m. In addition, a 30-m water level variation was formed by annual reservoir regulation. As a result of the combined effect of the large water level variation, relocation, and other factors, the geological conditions in TGR have been significantly changed, and challenges in terms of geological hazards prevention have been encountered in the Yangtze River. This paper focuses on the spatiotemporal distribution characteristics of landslides in six periods of 175 m ASL trial impoundments from 2008 to 2014. The mechanisms of reactivation of typical landslides in combination with reservoir water level variation, precipitation, and landslide monitoring data are analyzed. A detailed analysis of the difference between impulsive wave disasters generated by landslides in TGR before and after reservoir impoundment is conducted. Finally, the relationship between the variation in water level and landslide occurrence is discussed, and suggestions for the water level variation index are proposed on the basis of reservoir-induced landslide risk control.

2. Characteristics of landslides caused by 175 m ASL trial impoundment

In September 2008, the first trial impoundment at 175 m ASL was conducted in TGR according to the normal level of designed reservoir water storage. Based on experiences gained from most reservoir impoundments worldwide, old landslide reactivation and new landslide occurrence may be caused by reservoir impoundment and water level variations (Trzhtsinskii, 1978; Schuster, 1979; Wang et al., 2008a; Pinyol et al., 2012; Xiao et al., 2013; Guo et al., 2015). In this section, the spatiotemporal distribution rules of the landslide occurrence in the 175 m ASL trial impoundment are analyzed.

2.1. Temporal distribution characteristics of reservoir-induced landslides

From September 2008 to August 2014, TGR was subjected to 175 m ASL trial impoundment for six times (see Fig. 1 and Table 1). The maximum water level at the front of the dam site in 2008 and 2009 was 172.8 m and 171.4 m ASL, respectively; the maximum water level at the front of the dam site in 2010–2013 was 175 m ASL.

Table 1 shows the duration, overall variation, and average variation of the water level during each regulation. A large number of old landslide reactivations and new landslide occurrences were reported in the first 175 m ASL trial impoundment due to water level variations. The Liangshuijing landslide was one of the reactivation landslides during this period (Tan, 2011), which is an old landslide accumulated by ancient bedding rock mass sliding with a total volume of about 4 × 10^6 m^3. On 22 November 2008, the water level was elevated to 171.49 m ASL, and this landslide was reactivated. Large deformation and circular cracks were observed, which extended from the trailing edge to the Yangtze River side. The buildings hosted on the landslide body were severely damaged, and 55 people from 11 families in the landslide area were evacuated in an emergency. On 12 April 2009, after the water level decreased to 160.2 m ASL, the landslide deformation was once more increased, and navigation on the Yangtze River was blocked for several days. During the same period, several new landslides were observed, including Gongjiafang landslide. At the entrance to Wu Gorge on the left bank of the Yangtze River in Wushan County, Gongjiafang slope is a reversed bedding rock slope that mainly consists of medium to thin bedded limestone (Huang et al., 2012). On 23 November 2008, after the water level reached 172.8 m ASL, the first sliding occurred in Gongjiafang with a collapsing volume of about 380 × 10^3 m^3, which formed a 13-m high surge. On 18 May 2009, after the water level decreased to 150.5 m ASL, the slope recollapsed with a volume of about 15 × 10^3 m^3.

Old landslide reactivation and new landslide occurrence have a close relation with the process of water level variation. In general, during the six periods of the 175 m ASL trial impoundment, 328 landslides were reported in the reservoir region (Fig. 2), and the total volume of these landslides was about 350 × 10^6 m^3, of which 273 landslides (83.2%) were caused by the first water level variation process from 1 September 2008 to 31 August 2009. After the experiences in the first impoundment, the average daily water level increase was decreased in the subsequent 175 m ASL trial

Table 1
Water level variations in 175 m ASL impoundment and water level drawdown during six trials.

Period No.	Impoundment				Drawdown			
	Date	Duration (d)	Total fluctuation (m)	Average fluctuation (m/d)	Date	Duration (d)	Total fluctuation (m)	Average fluctuation (m/d)
1	28 September 2008 to 4 November 2008	37	27.53	0.744	13 November 2008 to 19 June 2009	218	27.59	0.127
2	15 September 2009 to 24 November 2009	70	25.56	0.365	25 November 2009 to 19 June 2010	206	26.21	0.127
3	10 September 2010 to 6 October 2010	46	14.8	0.322	1 January 2011 to 5 July 2011	185	29.55	0.16
4	10 September 2011 to 30 October 2011	50	22.76	0.455	1 January 2012 to 15 July 2012	166	29.34	0.177
5	10 September 2012 to 30 October 2012	50	15.72	0.314	24 December 2012 to 15 July 2013	173	29.34	0.17
6	10 September 2013 to 12 November 2013	63	17.88	0.283	13 December 2013 to 16 June 2014	185	28.76	0.156

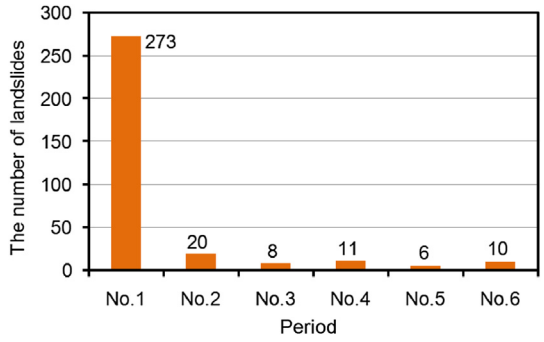

Fig. 2. Statistical graph showing the number of landslides induced by 175 m ASL trial impoundment and drawdown.

impoundments, whilst the average daily drawdown of the reservoir water level was slightly increased (Table 1). In addition, the number of reservoir-induced landslide occurrence decreased dramatically, from 273 landslides in the first 175 m ASL trial impoundment period to a few dozen in the second to sixth periods of the 175 m ASL trial impoundment. It should be noted that the number of reservoir-induced landslides in the last two periods of the 175 m ASL trial impoundment was not larger than 10.

Of the 328 landslides in the TGR region, there were about 109 (33.2%) new landslides. Reservoir-induced landslides can be divided into two types. The first type appears suddenly as landslide deforms or cracks at the initial stage, in the form of ground fracturing, small collapse, and large settlement. After that, it continues to deform slowly, such as Qingshi landslide in Goddess Stream (Lai et al., 2015). The second type appears in the form of rapid failure, such as Gongjiafang landslide (Huang et al., 2012). According to the survey in 2009, 1946 landslides were impacted by the impoundment of TGR. It can then be roughly inferred that the six periods of the 175 m ASL trial impoundment led to excessive deformation or failure, i.e. accounting for 16.9% of landslides in total.

In the process of the first trial impoundment, reservoir-induced landslides were concentrated on the period when the water level rose to above 160 m ASL. After the water level decreased slowly, the number of landslides increased continuously until the water level decreased to 145 m ASL in June 2009 (Fig. 1). During the second and third trial impoundments (175 m ASL), landslides mainly appeared in two periods: the period after the water level rose above 160 m ASL and the period of sharp variation of the water level in the summer flood season. Since the 4th 175 m ASL trial impoundment, reservoir-induced landslides were mainly observed in the period of water level decrease, with a few landslides randomly distributed.

The mechanism of landslide occurrence triggered by the 175 m ASL trial impoundment in the TGR region matches with that of the reservoir-induced landslides in other mountainous reservoirs. The initial impoundment period is characterized by a high possibility of landslides; as time elapses, the landslide occurrence shows a decreasing trend (Schuster, 1979) when the variation of the water level in the reservoir region is smaller than that at the initial stage, and in the condition that the measures for landslide prevention and reservoir protection will be subsequently enhanced.

2.2. Spatial distribution characteristics of reservoir-induced landslides

Fig. 3 shows the locations of landslides induced by the six periods of the 175 m ASL trial impoundments. From a geographical perspective, reservoir-induced landslides are mainly distributed along the main stream regimes and some branches of the Yangtze River. Because of the remarkable difference in the geological conditions of the slopes along the Yangtze River, a major difference in the landslide occurrences in various sections is observed. In this case, the TGR region can be divided into three sections in terms of landslide occurrences according to the geological conditions.

(1) Lower reservoir section

The broad valley section in the lower mountains and hills composed of crystalline rocks from the dam site to Miaohe is 16 km long (I in Fig. 3). It is composed of granite in the Pre-Sinian Period of the Huangling anticline core, and the topography is gentle and evenly distributed on both reservoir banks with a broad valley. There is a minor possibility of large-scale landslide development; only one large-scale landslide in this section was recorded, i.e. the Yemaomian landslide. On the north shore of the gorges between Niuganmafei Gorge and Konglingtan, this landslide is located 17 km away from the dam site of TGR, with a sliding mass volume of about 1.68×10^6 m^3. Monitoring results show that there is no visible displacement change in the Yemaomian landslide mass. Local monitoring points of the landslide mass change slightly in the water level increase and drawdown periods of the reservoir. However, the deformation direction of these points is not consistent. Currently, the landslide mass is essentially in a stable state (Yang et al., 2008, 2012).

(2) Middle reservoir section

The section composed of carbonate rocks interbedded with clasolite rocks from Miaohe to Baidi Castle is 141.5 km long (II in

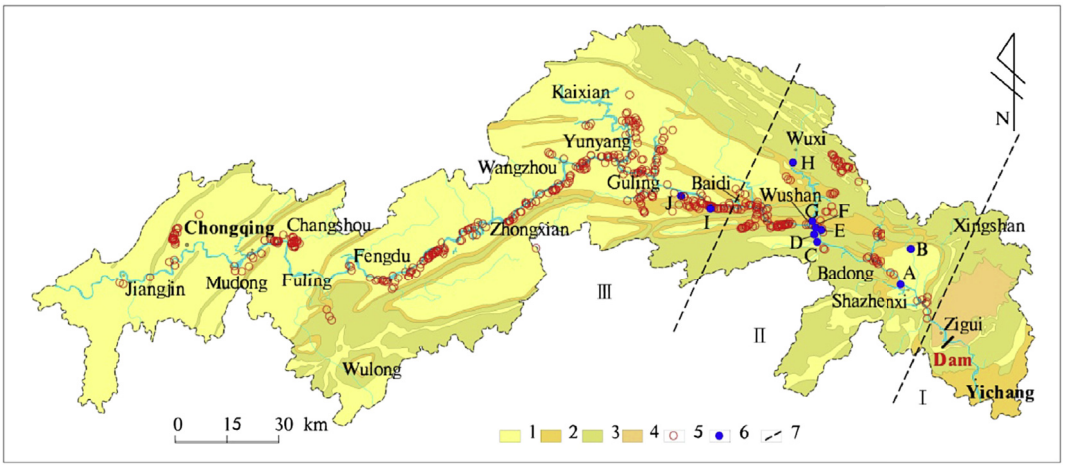

1. sandstone, shale and coal strata; 2. mudstone mixed with sandstone and shale; 3. limestone, dolomite interbedded with shale; 4. granite; 5. reservoir-induced landslides in six periods of the 175 m ASL trial impoundment; 6. nine landslides emphatically described in the paper; 7. section line of the reservoir region; A. Shuping landslide; B. Nierwang landslide; C. Qingshi landslide; D. Ganjingzi landslide; E. Wangxia collapse; F. Gongjiafang landslide; G. Hongyanzi landslide; H. Chuanzhu landslide; I. Outang landslide and Anping Town; J. Liangshuijing landslide.

Fig. 3. Distribution map of landslides induced by six periods of the 175 m ASL trial impoundment (from 1 September 2008 to 31 August 2014).

Fig. 3). This section shows alternating landforms of gorges and broad valleys, which belong to the Qianjiang arch fold-faulted bundle of the Yangtze platformal fold belt in tectonic setting. In the six periods of the trial impoundments, reservoir-induced landslides developed mainly from Qingshi of Wushan County to Baidi Castle of Fengjie County. The geological conditions in this region are complex, with continuous exposure of formations from the Silurian System to the Triassic System. The strata in the gorge area mainly include limestone and dolomite, and in the broad valley mudstone, sandstone, and shale interbed are mainly included. Rockfalls and landslides are relatively well developed in this section. The Gongjiafang landslide and Wangxia rockfall are located in this gorge area.

The region from Shazhenxi Town of Zigui County to Badong County is also susceptible to landslides. However, since this region is close to the head of the reservoir, the reactivation of new and old landslides occurred mainly in the periods of impoundments between 2003 and 2007 at 135 m and 156 m ASL. The bedrock formation exposed in the region mainly includes the Badong formation in the Triassic System and Jurassic System, and they are sliding-prone strata in the TGR region. The Qianjiangping landslide (Wang et al., 2008a), Shuping landslide (Wang et al., 2008b), and other large-scale landslides occurred in this region.

(3) Upper reservoir section

The clasolite rock section from Baidi Castle to Maoer Gorge in the reservoir tail is 492.5 km long (III in Fig. 3). This section shows broad valleys in low mountains and hills in landform, and it belongs to the Chuandong fold belt in the depression of the Sichuan Platform in tectonic setting. In the six periods of the trial impoundment, reservoir-induced landslides were mainly developed in the region from Anping Town of Fengjie County to Guling Town of Yunyang Country, in the region from the town site of Yunyang Country to Fengdu County, and in the region from Changshou District to Mudong Town. The strata exposed in the section are mainly of mudstone, siltstone, and sandstone interbedding in the Jurassic system, which are mainly composed of medium-to-low dip slopes. Typical landslides, such as the Liangshuijing landslide and Fengbaoling landslide, occurred in this section.

3. Mechanism of typical landslides in 175 m ASL trial impoundment

The statistics of 60 reservoir-induced landslides indicate that 85% occur within the storage period or two years after project completion (Riemer, 1992). Analysis of more than 100 landslides in 50 reservoirs from six countries shows that about 75% reservoir-induced landslides are reactivations of old landslides (ICOLD, 2002). Among the landslides induced by six periods of the 175 m ASL trial impoundment in the TGR region, old landslide reactivation accounted for 66.8%; some large-scale landslides were found in nature to be reactivations of old landslides. In view of landslide materials and slope structures, reservoir-induced landslides in the TGR region can be classified into five failure patterns, including accumulation landslide, dip-slope landslide, reversed bedding landslide, rockfall, and karst breccia landslide (Yin, 2005). Accumulation landslides and dip-slope landslides account for more than 90% of total landslides (Li et al., 2007; Lu, 2011; Xin, 2012). Therefore, this paper will focus on accumulation landslides and dip-slope landslides to understand the mechanism of deformation and failure under water level variation and precipitation conditions.

3.1. Mechanism of accumulation landslide reactivation

The mass of accumulation landslide in the TGR region is mainly composed of rock sliding deposits. The permeability of loose mass is relatively high, while the permeability of cataclastic stone with original rock structure is relatively low. In general, the sliding zone is saturated or wetting, and has greater silt content and relatively lower permeability, which forms a relatively impermeable layer of slope (Highland and Bobrowsky, 2008; Liu, 2011; Tang et al., 2012).

The accumulation landslide reactivation in the TGR region is generally related to the annual regulation of reservoir impoundment and the precipitation during the flood period. Taking Shuping accumulation landslide for example, the stability under coupled water level variation and precipitation is analyzed in order to reveal

the primary reactivation mechanism of typical accumulation landslides.

3.1.1. Overview of Shuping landslide

Shuping landslide is located on the south bank of the Yangtze River in Zigui County of Hubei Province (point A in Fig. 3). The elevations of the crown and the toe of the landslide are 470 m and 68 m ASL, respectively (Fig. 4). The north-to-south length is about 800 m, and the east-to-west width is about 670 m. The landslide mass is 10–74 m in thickness. The landslide area is about 541×10^3 m^2, and the total volume is about 20.7×10^6 m^3. The landslide materials mainly include gravelly soil and cataclastic stone accumulated by ancient sliding. The sliding surface mainly consists of brown breccia soil and silty clay (Fig. 5). The sliding bed is composed of medium bedded siltstone mixed with mudstone (T_2b), and medium bedded limestone and muddy limestone in the middle Badong formation of the Triassic System. In general, landslide topography is characterized by alternating steep slope and gentle slope. The slope angle of the landslide is 5°–35°.

After impoundment was launched in the TGR region in June 2003, Shuping landslide continuously deformed. From 2008 onward, the landslide deformation was larger when the water level decreased from the maximum water level to the minimum in the annual flood season. It can be seen from the displacement curves that this landslide had three steps of deformation periods in 2009, 2011 and 2012 (Fig. 6). In late May 2009, severe deformations appeared, and the maximum deformation rate recorded by the measuring points reached 18.47 mm/d. Excessive deformations were also observed in 2012. On 11 June 2012, the maximum deformation rate of the surface measuring point exceeded 15 mm/d, and the cracks around the landslide were further extended and widened (3–20 cm in width and 518 cm in settlement). The east ruptures further developed basically in en echelon arrangement, which had formed seven shallow collapses and 11 tensile fractures.

In order to record the deformations, four displacement monitoring holes, i.e. QZK1, QZK2, QZK3, and QZK4 (see Fig. 4), were used for Shuping landslide. From the monitoring curves of the borehole inclinometers in 2012, the landslide experienced significant displacement along the sliding directions (see Fig. 7). The monitoring curves of QZK1 and QZK3 show that the depths of the monitoring holes in the sliding zone are 20 m and 70 m, respectively. In addition, it can be seen that the landslide underwent continuous deformation, and the average displacement rate of the deep underground borehole is 0.1–0.26 mm/d from February to March in 2012. As the deformation of the landslide continued, the borehole inclinometers were out of the measuring range and were unfortunately damaged.

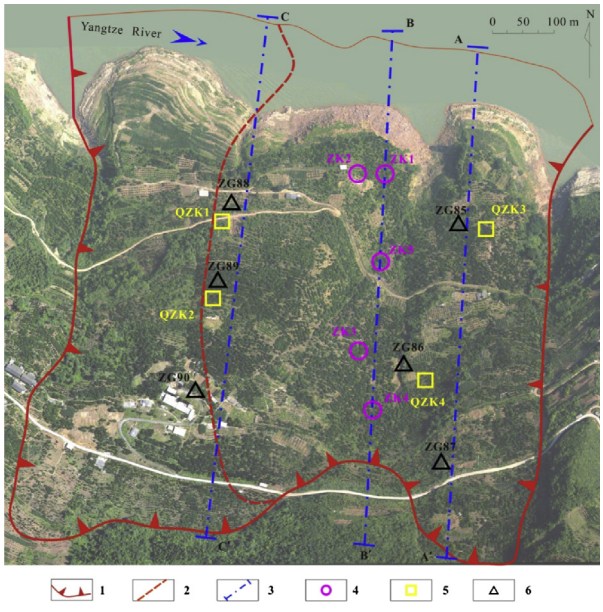

1. landslide boundary; 2. secondary boundary of landslide; 3. section line; 4. borehole; 5. deep inclinometer borehole; 6. ground displacement monitoring point.

Fig. 4. Monitoring plan for Shuping landslide of Zigui County, Hubei Province. The remote sensing image was taken in June 2009; the water level was about 145 m ASL.

3.1.2. Relationship between reservoir water level variation, precipitation and factor of safety

According to the monitoring data of the groundwater level boreholes on the toe of the landslide, there is a positive correlation between the overall deformation trend of the landslide and the groundwater level variation. When the gradient of the groundwater level is close to 0, the landslide deformation rate is smaller than 1 mm/d. When the gradient decline of the groundwater level is close to 0.015, the landslide deformation rate reaches the high value of 7.3 mm/d.

In terms of factor of safety (FOS) calculation, Morgenstern and Price (1965) proposed a strict limit equilibrium stability analysis method for a sliding surface of arbitrary shape. Chen and Morgenstern (1983) modified the Morgenstern-Price method by the improved universal bar method, and proposed calculation formulae of a number of derivatives required by Newton–Raphson iterations. This can ensure rapid convergence of the numerical calculation in most cases. To understand how water level variation influences the landslide stability, quantitative analysis was conducted by Geo-Studio software with the traditional coupling method of the Morgenstern-Price method with the SLOPE/W module and seepage analysis with the SEEP/W module (Geo-Slope International, Ltd., 2008a, b). First, the steady-state condition was considered to be the initial condition for the next transient analysis, in which the water level variation and precipitation were included. SLOPE/W is able to read the transient seepage results directly from SEEP/W in order to compute the actual pore water pressures at the base of each slice. Finally, the FOS of the landslide was calculated under the transient-seepage condition.

Table 2 lists the physico-mechanical parameters adopted in the calculation, which were obtained from the experiment. With the saturated physico-mechanical and hydraulic parameters of the landslide mass, the initial seepage field of groundwater on 1 September 2008 could be established by fixed water heads in the boundary conditions in a steady-state analysis, and then the transient seepage analysis was conducted at a specific time step for an actual water level process and the actual precipitation process from September 2008 to July 2014.

When only water level variation was considered, the numerical result shows that the water level decrease in the reservoir greatly impacted Shuping landslide. When the reservoir water level decreased, the FOS of Shuping landslide reduced rapidly (Fig. 8). In the first water level drawdown in 2008, the water level was decreased by 5 m from the end of October to the end of December, but the FOS of Shuping landslide decreased rapidly from 1.12 to 1.05. This occurred because the water level drawdown inside the landslide basically lagged behind the reservoir water level, and the instability tendency of the landslide was caused by the difference between the internal pressure and the external pressure (Terzaghi, 1944; Lane and Griffiths, 2000; Berilgen, 2007).

Considering the coupling effect of water level variation and precipitation, the FOS is smaller than the one calculated by only considering water level variation. At the end of May 2011, the calculated FOS of Shuping landslide was only 0.99. Since nearly 50%

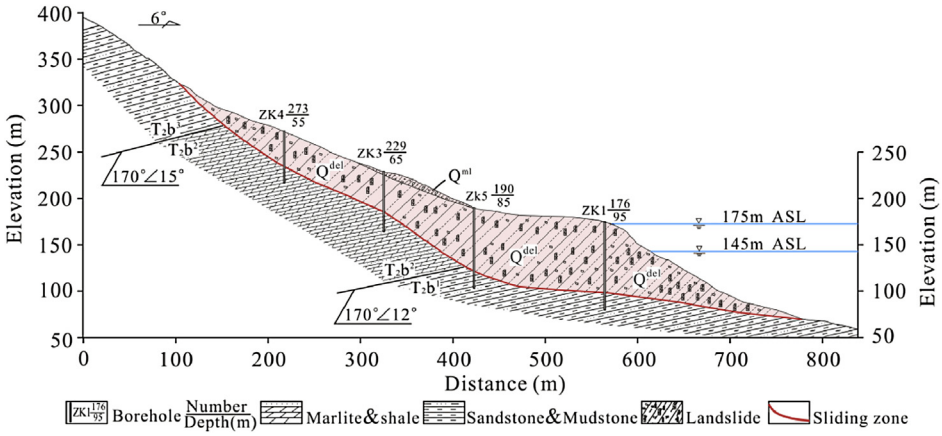

Fig. 5. Engineering geological section B–B' of Shuping landslide of Zigui County, Hubei Province.

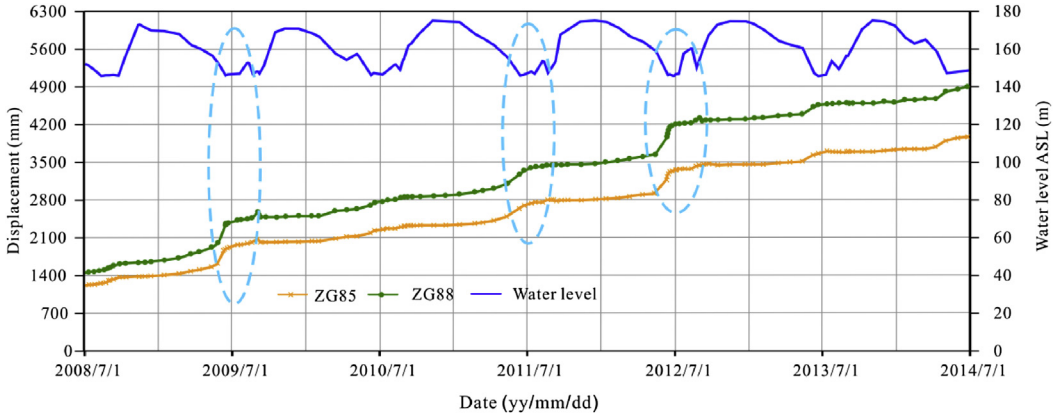

Fig. 6. Monitoring curves for ground displacement of Shuping landslide of Zigui County, Hubei Province in six 175 m ASL trial impoundments (data recorded from 1 July 2008 to 1 July 2014).

of the landslide mass is located above the water level of 175 m ASL in Shuping landslide, the sliding surface of the upper landslide mass will be saturated as a result of continuous rainfall seepage, and the slope stability will be further decreased. Accumulation of rainfall seepage will also contribute to the slope instability (Hu et al., 2015).

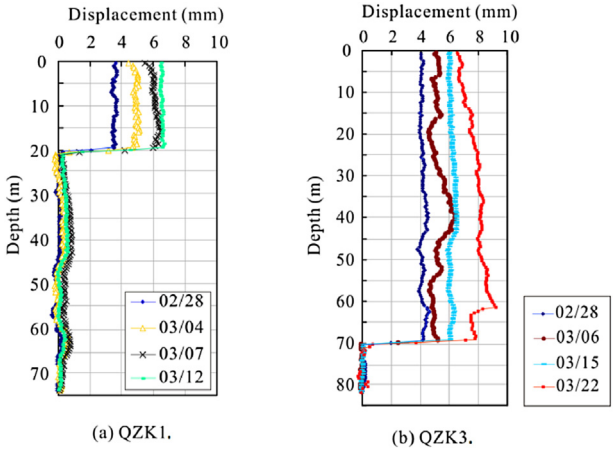

Fig. 7. Monitoring curves for deep inclinometers of Shuping landslide in Zigui County, Hubei Province (monitoring data recorded from February to March, 2012).

According to the relationship between FOS, water level variation and precipitation, the FOS appears to lag behind the water level variation. After considering precipitation, the maximum FOS decrease of the landslide is only 5%. Therefore, the reservoir water level is regarded as a major factor accounting for Shuping landslide, and the landslide stability may be affected slightly by accumulated precipitation seepage.

The coupling analysis from 2008 to 2014 indicates that the global stability of Shuping landslide will be gradually reduced, and the FOS will be lower than the limit state values in a global sense, and then it will fail.

3.1.3. *Triggering factors of accumulation landslide reactivation*

The main triggering factor of Shuping landslide reactivation is water level variation. During the process of water level drawdown,

Table 2
Main physico-mechanical and hydraulic parameters of Shuping landslide.

Material	Unit weight (kN/m^3)	Elastic modulus (MPa)	Poisson's ratio	Saturated shear strength		Hydraulic conductivity (m/s)
				Cohesion (kPa)	Internal friction angle (°)	
Sliding mass	21.1	25	0.35	20	18	2.8×10^{-5}
Sliding zone	20.5	12	0.36	15	12	2.3×10^{-7}
Bedrock	24.5	2.5×10^4	0.22	1500	45	0

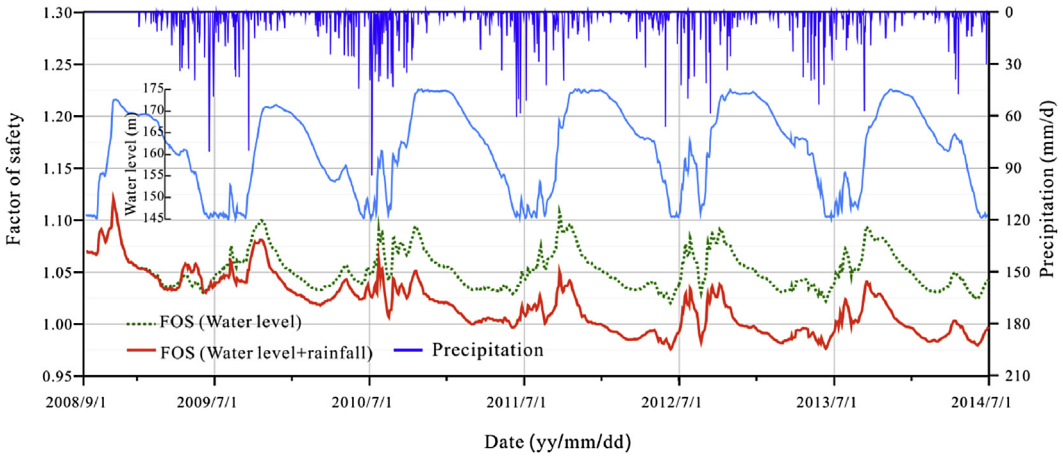

Fig. 8. Evolution of FOS of Shuping landslide in Zigui County, Hubei Province, under effect of water level and precipitation (data recorded from 1 September 2008 to 1 July 2014).

the FOS of the landslide decreased rapidly, and the landslide was subjected to severe deformation (Duncan et al., 1990; Wang et al., 2008b). Therefore, the landslide deformation curve will show a step-shaped profile along with the periodic rising and drawdown of water level.

The hydrologically triggered accumulation landslides are initiated by variation in pore water pressure on the potential slip surface and reduction of the shear strength parameters. For accumulation landslides such as Shuping landslide, the FOS analysis indicates that the main triggering factor is water level variation (Breth, 1967; Kim et al., 2010; Rodríguez-Peces et al., 2011; Prokešová et al., 2013; Zhao et al., 2015). The reactivation and deformation mechanisms of many large-scale old landslides in the TGR region, such as Baijiabao landslide and Baishuihe landslide, are similar to that of the Shuping landslide, and their deformation curves are similar to those of Shuping landslide (Chen and Huang, 2006; Huang and Chen, 2007; Li et al., 2010).

Concerning the triggering factors, there are generally two major periods for the occurrence or reactivation of accumulation landslides in the TGR region. One is the initial impoundment period, especially at high water level. As a result of the water level increase in the reservoir, the volume of the soaked mass of the slope increases, the effective stress or sliding resistance force on the sliding surface decreases, and the strength of some sliding zones decreases subsequently, which may easily cause slides (Liu, 2011). For example, the Changzheng landslide in Hefeng Town occurred on 9 November 2008, and the reservoir water level rose to 172.6 m in the first period. The other is the water level drawdown period, especially rapid water drawdown. When the reservoir water level drops suddenly, the drawdown of the groundwater level within the slope (especially near the sliding zone) lags, and excessive pore water pressure is produced, which may lead to slope instability (Terzaghi, 1944; Lane and Griffiths, 2000; Berilgen, 2007). For example, Huanglianshu landslide occurred on 31 May 2012, when the water level dropped to 153.2 m ASL.

3.2. Mechanism of dip-slope landslide deformation and failure

The dip-slope landslides in the TGR region tend to occur in interbedded stratum of muddy limestone, sandstone and mudstone. The sliding zone of dip-slope rockslide is mainly developed in soft layers, such as mudstone, shale and coal-bearing layer (Li et al., 2007). The sliding bed of dip-slope landslides may extend to a large scale, which is favorable for groundwater seepage. Deformation of dip-slope landslides is usually associated with the seepage field of groundwater and the annual regulation of the reservoir.

Taking Outang large-scale dip-slope landslide for example, the stability under the coupled reservoir variation and precipitation was analyzed in order to reveal the mechanism of deformation and the failure of typical dip-slope landslides.

3.2.1. Overview of Outang landslide

Outang landslide lies on the south bank of the Yangtze River, Anping Town of Fengjie County, Chongqing (Fig. 9). The maximum width, up to 1100 m, of the landslide is distributed along the shore of the Yangtze River. The crown and toe elevations of the landslide are about 705 m and 95 m ASL, respectively. The maximum length of the landslide is about 1800 m, and the area covers about 1.78 km^2. The average thickness of the landslide mass is about 50.8 m, and the volume is about 90×10^6 m^3. The main sliding direction of the landslide is 340°–350°. The landslide mass mainly consists of silty clay mixed with gravel and cataclastic stone. The sliding zone is composed of black clay. The sliding bedrock is sandstone with good integrity, which shows weak water permeability (see Fig. 10).

After the first 175 m ASL trial impoundment, more than 160 cracks were observed in the Outang landslide region; the number of new cracks reached a peak, especially in the first drawdown period of the water level. The monitoring data since December 2010 indicate a significant displacement in the Outang landslide (see Fig. 11). However, there is a weak correlation between the deformation of the landslide and the water level increase. The average rate of the reservoir water level increase reaches the maximum value from October to November each year, but the average rate of landslide displacement shows a small variation. The 60%–70% displacements mainly take place from May to September each year. Taking the monitoring point MJ08 for example, the total displacement from May to September each year reached 207.97 mm during the last 5 years, and the total amount of displacement deformation in other time periods was only 87.55 mm; similar deformation rules exist in other monitoring points (see Fig. 12).

Fig. 11 shows that, from the cumulative displacement curves, two prominent accelerated deformations of the landside appeared in 2012 and 2014 (ellipse areas). Such accelerated deformation is closely related to heavy precipitation. In fact, the precipitation in May 2012 reached 275 mm, and the displacement deformation at the monitoring point TN03 was 25.62 mm/month. The precipitation in September 2014 reached 312 mm, which was considerably higher than the precipitation in the same month during the past 5

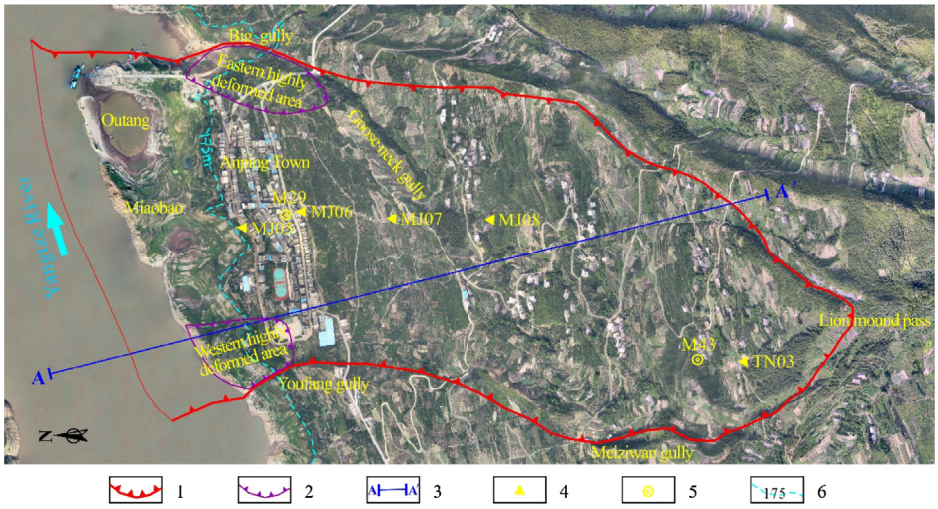

1. landslide boundary; 2. local shallow landslide boundary; 3. section line; 4. ground monitoring site; 5. inclinometer borehole; 6. water level of 175 m ASL.

Fig. 9. Monitoring plan of Outang landslide in Fengjie County, Chongqing. The remote sensing image was taken on 10 July 2013, and the water level was 144.2 m ASL.

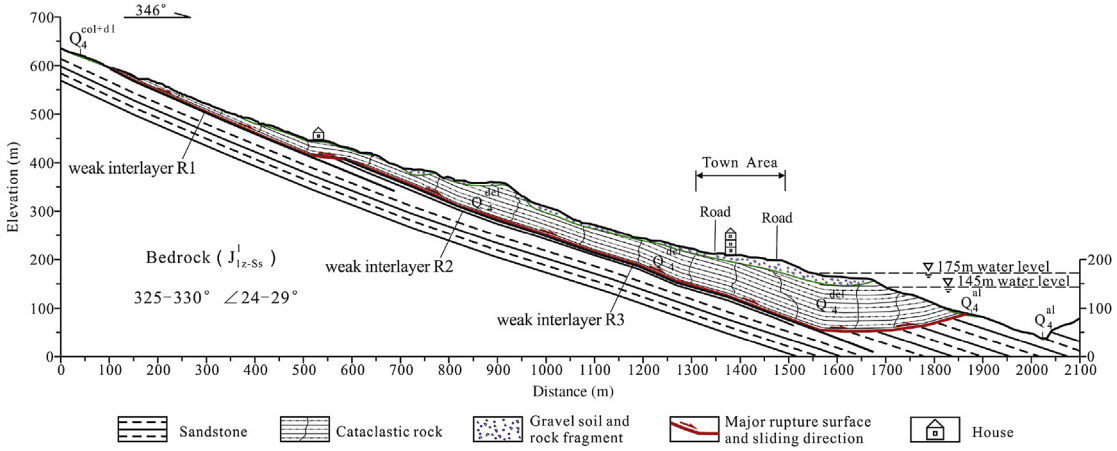

Fig. 10. Engineering geological section *A*–*A*′ of Outang landslide of Fengjie County, Chongqing.

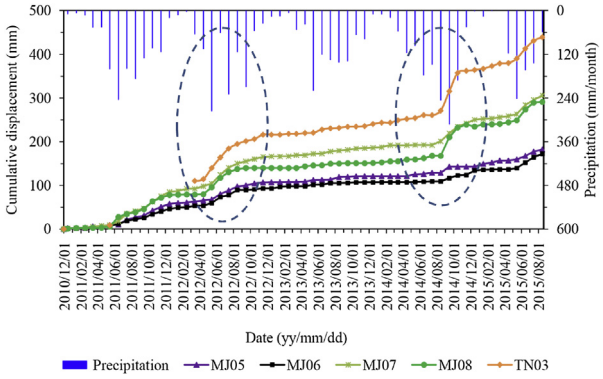

Fig. 11. Relationship of cumulative ground displacement, reservoir water level and rainfall in Outang landslide in Fengjie County, Chongqing.

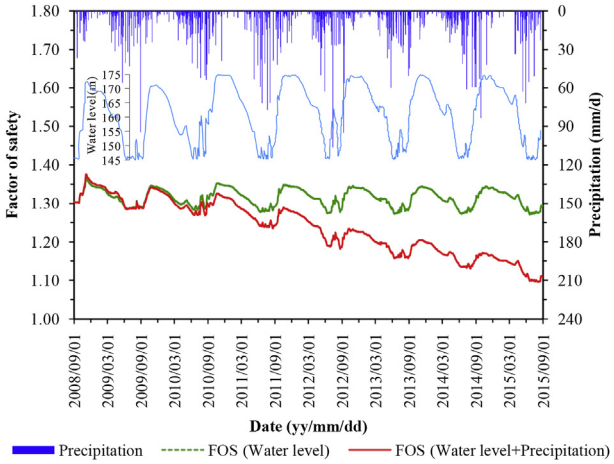

Fig. 12. Evolution of FOS of Outang landslide under effect of reservoir water level and precipitation.

years. Landslide displacement shows a significant increasing trend. Especially for monitoring points MJ08 and TN03 at the middle and rear parts of landslide, the monthly displacements are 42.66 mm and 44.55 mm, respectively. Clearly, precipitation is an important factor influencing the stability of Outang landslide.

3.2.2. Relationship between reservoir water level variation, precipitation and factor of safety

The FOS of the Outang landslide was calculated using the same procedure as mentioned for the Shuping landslide analysis. Table 3 lists the physico-mechanical and hydraulic parameters of Outang landslide mass, which were obtained from experiments.

When merely considering the variation in reservoir water level, the groundwater level in Outang landslide under the reservoir water level of 175 m ASL was obviously higher than that of 145 m ASL. The change in the groundwater level from the toe to the crown influenced by the reservoir water level variation was characterized by a gradual decrease, and the groundwater level at the rear part of the landslide above 350 m ASL showed a smaller variation. This fact is consistent with the analysis results of the monitoring data for groundwater in the landslide site.

The seepage field of groundwater was analyzed under two conditions, i.e. reservoir variation and reservoir variation coupled with precipitation. It was found that the seepage in the landslide mass under reservoir variation coupled with precipitation was obviously higher than that when only considering reservoir water level variation. The groundwater level in the landslide increased to a certain degree as a result of continuous precipitation, which was negative with respect to landslide stability. In view of short-term intensive precipitation, we took the pore water distribution of the sliding mass on 23 June 2011 (rainfall on that day was 72.2 mm) for example. Due to intensive precipitation and low permeability of the landslide mass, a transient saturated zone was formed on the surface of the landslide mass. With respect to regions less affected by reservoir water at the rear part of the landslide, the underground seepage field varied significantly. As a result, the shear strength of the mass at the rear part was reduced, local stability was decreased, and the sliding force of the global sliding mass increased (Fredlund and Rahardjo, 1997).

When only considering the reservoir water level variation, the FOS of the landslide will change with reservoir water level, and tends to decrease gently as time elapses. Similar to the Shuping landslide, considering the coupling effect of water level variation and precipitation, the FOS is smaller than that calculated by only considering water level variation. The smaller FOS often appears in the period of rapid drawdown of the water level and continuous heavy rain (from May to July every year). Basically, the calculated FOS of Outang landslide is 1.1–1.36. When water level variation and precipitation are considered, the FOS is greater than 1, suggesting that this landslide is basically in a stable state, which is almost identical to the current situation of the landslide.

Basically, the evolution of FOS lags behind the water level variation as well as precipitation, similar to Shuping landslide. When taking the precipitation into account, the FOS of Outang landslide is decreased by about 18%. Therefore, it is assumed that the reservoir water level and precipitation seepage are both the major factors influencing the stability of Outang landslide.

Stability analysis also shows that, as periodic variation of water level and precipitation seepage increases, the stability of the global landslide declines gradually. This endangers a large number of residents living in the landslide mass area (including Anping Town). Under this circumstance, the residents on the landslide mass began to relocate in October 2014.

3.2.3. Triggering factors of dip-slope landslide deformation and failure

It is known that the Outang landslide deformation has a close relationship with water level variation as well as intensive precipitation. The mechanism of water level variation on dip-slope landslides is similar to that on accumulation landslides. As a result of precipitation seepage, when pore water pressure in rock-soil mass increases, the matric suction decreases accordingly. Under continuous precipitation, the landslide state transforms from unsaturated to saturated; thus, the shear strength of the sliding zone and sliding mass are weakened (Fredlund and Rahardjo, 1997; Collins and Znidarcic, 2004; Crosta and Frattini, 2008). The dip-slope region is susceptible to landslides, due to its unstable geo-structure. This geo-structure is beneficial for the formation of sliding forces on the slide mass along the flat and straight sliding bed, especially the pore water pressure (Ghimire, 2011; Santangelo et al., 2015). A flat and straight sliding bed is a relatively impermeable layer. Thus, when in contact with rainfall seepage, buoyancy pressure (uplift pressure) or excessive pore water pressure will be induced in the same direction near the sliding zone, leading to the instability of the landslide mass.

In terms of bedding slope structure and straight sliding bed, old dip-slope landslides are easily reactivated under the combined effect of reservoir water and precipitation (Tang et al., 2015). Water level variation and precipitation will reduce the FOS of the Outang landslide, which are the major triggering factors of reactivation of this landslide. The reactivation mechanism of many large-scale dip-slope landslides in the TGR region is similar to that of Outang landslide. For example, Fengbaoling landslide occurred on 7 March 2011, which is also a dip-slope landslide composed of mixed rock and soil. It occurred when the reservoir water level dropped to 165.11 m ASL, and there had been strong rainfall a few days before. Nierwang landslide occurred on 5 November 2008, which is a typical accumulation dip-slope landslide. It occurred when the water level rose to 172 m ASL, and the precipitation that occurred 3 d before was 24.4 mm (Tian and Lu, 2012).

Table 3
Main physico-mechanical and hydraulic parameters of Outang landslide mass.

Material	Unit weight (kN/m^3)	Elastic modulus (MPa)	Poisson's ratio	Saturated shear strength		Hydraulic conductivity (m/d)
				Cohesion (kPa)	Internal friction angle (°)	
Silty clay mixed with pebbly clay	20.5	20	0.32	16	14.6	1.05
Cataclastic rock mass	26	420	0.25	70	16.2	0.26
Sliding zone	21	115	0.33	8	16.5	0.05
Bedrock	27.6	1.6×10^4	0.2	700	42	0.003

4. Impulsive wave risk generated by landslide after 175 m ASL trial impoundment

Before the failure of Gongjiafang landslide on 23 November 2008, the main landslide concerns in TGR were the deformation, failure mechanism, monitoring, forecasting and prevention. The main factor that determines whether a landslide is treated is based on the potential losses resulting from the landslide and its coverage along the slope area. Minor attention has been paid to the impulsive wave generated by landslides. However, impulsive waves may be generated by reservoir-induced landslides, which endanger towns and shipping over a long distance along the river. In October 1963, Vajont landslide occurred in Vajont reservoir of Italy with a sliding

mass volume of up to 270 × 10^6 m^3, generating huge surge overtopping the dam, which killed 1925 people in the downstream region (Müller, 1964; Bosa and Petti, 2013). Since the 175 m ASL trial impoundment in 2008, impulsive wave disasters have occurred in the TGR region for many times, posing a significant threat to the safety of the Yangtze River channel and immigrant towns. Therefore, scientific evaluation and suitable risk management of landslide-induced impulsive waves are the major tasks of reservoir-induced landslide risk control in the reservoir region. This paper will compare the difference in landslide-induced impulsive wave disasters before and after the 175 m ASL trial impoundment, and the potential impulsive wave risks generated by landslides in the reservoir will be discussed.

4.1. Characteristics of landslide-induced surge disaster in TGR region

4.1.1. Before 175 m ASL trial impoundment

According to the records, impulsive wave events were caused by landslides in some sections of the mainstream and its tributaries in the TGR region, posing a huge threat to the local people. For example, in the second year of the Jin Dynasty (AD 377), a collapse in Wushan County blocked the river and generated adverse currents. The largest surge was about 20–30 m high. Before the 175 m ASL trial impoundment, only three landslides generated a large impulsive wave among more than 70 landslides in the TGR region from the 1980s to 2008 (Table 4) (Li, 1984; Liu, 1987; Chen and Zhang, 1994; Yin et al., 2015).

The three impulsive wave-induced disasters shown in Table 4 have the following common characteristics: (i) landslide volume was millions to tens of millions of cubic meters; (ii) river water was tens of meters deep, and a landslide dam was formed since a large-scale mass blocked the water way; and (iii) a water wave of tens of meters high was caused by a landslide. Since the river depth during the three events was less than the length of the sliding mass body, occupation of landslide mass in the channel must be considered, which is typically a wave generated by landslides along a shallow water region. According to eyewitness's descriptions and analysis of landslide-induced surge cases (Basu et al., 2009; Pastor et al., 2009; Yin et al., 2015), and because the river is narrow, the generation, propagation and run-up of a surge generated by a landslide mixed together in the river course where the landslide was located. A water body will form a water tongue or water wall in a high-velocity motion, which may strike and apply a strong force to the opposite bank. The upstream and downstream regions of the channel were cut off or partially blocked by the landslide, and the hydraulic link between the upstream and downstream regions was totally or partially cut off.

4.1.2. During 175 m ASL trial impoundment

At the beginning of the 175 m ASL trial impoundment in 2008, the river depth was about 100 m, which provided a good condition for a reservoir-induced landslide to generate a surge after the water level increased. During the first 175 m ASL trial impoundment, three impulsive wave-induced disasters and four potential impulsive wave risks occurred in the reservoir (Table 5) (Huang, 2014). On 23 November 2008, the Gongjiafang landslide occurred in Wu Gorge, which was caused by reservoir impoundment. The landslide mass almost completely rushed into the river and caused a 13 m high surge (Huang et al., 2012).

There are differences between the characteristics of landslide-induced surge in the main stream before and after impoundment. The landslide-induced surge generated along a deep water area shows three typical phases: generation, propagation and run-up (Huang et al., 2012, 2014). Meanwhile, the volume occupation induced by the landslide mass blocking the channel can be ignored. It should be noted that the landslide-induced surge generated in the reservoir tail and some tributaries are still impulsive wave types along the shallow water region.

In general, the risk of landslide-induced surge hazards increased significantly after the 175 m ASL trial impoundment. Firstly, the possibility of landslide occurrence is higher after reservoir impoundment. For example, there were more than 70 landslides in the last 28 years prior to impoundment, but there were 328 landslides in the 6 most recent years after impoundment. Secondly, the slope toes of 65% of the landslides are under the water, and landslide movement will trigger water body movement directly. Thirdly, after impoundment, navigation in the Yangtze River increased dramatically due to the deep water tunnel, and most new immigrant towns are located on the bank of the Yangtze River. However, small- or medium-scale landslides may generate a huge water wave risk. For example, the volumes of the Gongjiafang and

Table 4
Summary of landslide and impulsive wave disasters generated by reservoir-induced landslides before 2008.

Date	Location	Description of landslide surge disasters
12 June 1985	Xintan landslide, Zigui County	With a total volume of 30 × 10^6 m^3, the landslide rushed into Yangtze River at a maximum speed of 31 m/s (Chen et al., 1985). The inrush volume to the river was about 2.6 × 10^6 m^3, which blocked Yangtze River and formed a 54 m high (maximum) surge, and thus influenced a 42-km-long section in the Yangtze River channel.
30 April 1994	Jiguanling collapse, Wulong County	Debris flow (5.3 × 10^6 m^3) was formed and entered Wu River, a tributary of Yangtze River. The inrush volume to the river was about 0.3 × 10^6 m^3, which blocked Wu River and generated an impulsive wave. As a result of a 10–15 m high impulsive wave, 5 boats were damaged, 4 people were killed, 12 people went missing, and 5 people were injured (Chen and Zhang, 1994).
13 July 2003	Qianjiangping landslide, Zigui County	The landslide volume was about 15 × 10^6 m^3, and the maximum sliding speed was 16 m/s (Xiao et al., 2013). The 2.4 × 10^6 m^3 mass blocked Qinggan River, a tributary of Yangtze River, and formed a surge with a maximum height of about 39 m. As a result, 22 fishing boats were damaged, and 13 people went missing.
16–17 July 1982	Jipazi landslide, Yunyang County	Jipazi landslide was induced by the effect of a strong rainstorm, with a total volume of 15 × 10^6 m^3. The volume of mass sliding to the river was 1.8 × 10^6 m^3, and the landslide blocked Yangtze River channel. Because the flood was caused by a rainstorm, the impulse wave phenomenon in Yangtze River was not as significant as expected (Li, 1984).

Table 5
Impulsive wave disasters generated by reservoir-induced landslides since 175 m ASL trial impoundment.

Date	Location	Description of landslide surge disasters
22 November 2008	Chuanzhu landslide, Wuxi County	The landslide had a total volume of about 1×10^6 m^3, and 0.1×10^6 m^3 mass rushed into Daning River. The landslide blocked a 1/4 channel cross-sectional area and generated a 4-m-high surge. As a result, navigation in the Daning River channel was affected and even closed.
3 November 2008	Gongjiafang landslide, Wushan County	The volume was 0.38×10^6 m^3, the maximum run-up was 13 m, and was about 1–2 m at Wushan County after a distance of 4.5 km. As a result of the surge, infrastructure and several boats along the 10-km-long bank were damaged; direct economic losses were about CN ¥5 million (or US $0.75 million).
9 November 2008	Nier Gulf landslide, Zigui County	With a total volume of about 0.8×10^6 m^3, the potential surge risk generated by this landslide endangered local residents and schools at elevations below 200 m in Shuitianba Town on the opposite bank. The residents and students were evacuated, and navigation in the Guizhou River channel was restricted and even closed.
12 March 2009	Liangshuijing landslide, Yunyang County	The total volume was about 3.6×10^6 m^3. The landslide mass was subjected to continuous deformation, and the potential surge risk limited navigation in the Yangtze River channel and resulted in huge economic losses.
21 October 2010	Wangxia collapse, Wushan County	After collapse, the potential surge risk restricted navigation and caused channel interruption, leading to huge economic losses.
11 October 2010	Qingshi landslide, Wushan County	The landslide is located in Goddess Stream, a tributary of Yangtze River. After severe deformation, the potential surge risk resulted in the closure of the Goddess Stream scenic spot for more than 1 year and led to direct economic losses of more than CN ¥100 million (or US $15 million).
24 June 2015	Hongyanzi landslide, Wushan County	Hongyanzi landslide is located on the opposite bank of Wushan County, which is a bedding soil landslide with a volume of 0.23×10^6 m^3. Impulse waves (5–6 m high) were generated, which overturned 13 boats, killed 2 persons, and injured 4 persons.

Hongyanzi landslides were 0.38×10^6 m^3 and 0.2×10^6 m^3, respectively, which are far lower than the volume of the landslides before impoundment. However, the impulsive wave triggered by two landslides resulted in disaster in Wushan County.

After impoundment, evaluation of potential landslide-induced surge is one of the major concerns for landslide risk prediction in the reservoir region. In November 2010, serious deformations were observed in Qingshi landslide in Goddess Stream, a tributary of the Yangtze River. Considering that a potential impulsive wave may lead to huge hazards in the Goddess Stream channel, a 1-year shipping suspension was conducted until landslide prevention and treatment were implemented. In recent years, early-warning of landslides with surge risks in the reservoir region has been strengthened, and positive prevention of geological hazards has been conducted on this basis.

4.2. Potential impulsive wave analysis of 175 m ASL trial impoundment

Potential impulsive wave risk analysis of reservoir-induced landslides is an important index to classify the hazards of landslide and evaluate the landslide risk. Taking the Ganjingzi accumulation landslide for example, the hazards of potential surges for individual landslides will be analyzed, and then the classification of potential landslide-induced surge risks in the reservoir will be proposed.

4.2.1. Overview of Ganjingzi landslide

Ganjingzi landslide lies at the entrance of Wu Gorge on the right bank of the Yangtze River in TGR (Fig. 13), and serious deformation was observed in June 2015. The elevation of this landslide crown is 390 m, where a tensile crack developed with a length of about 300 m. The toe is submerged below the water, and the elevation of the shearing outlet is about 135 m ASL. The landslide is about 440 m long, 220 m wide, 20–25 m thick and has a volume of about 2×10^6 m^3. A tensile crack developed at an elevation of about 240 m. The crack is about 50 m long, and the settlement is 15–20 cm with a width of 10–20 cm, which is the boundary of the crown characterized by the strongly deforming mass of the landslide. The length of the serious deforming mass is 170 m, the width is 100 m, and the area is 17×10^3 m^2. The average thickness is about 12 m, and the volume is about 200×10^3 m^3. The sliding mass material is composed of gravelly soil, and the dip angle of the landslide is 350°. The underlying bedrock is shale in the second section of the middle Luoreping group in the Silurian system (S_2lr^2) with an attitude of 330°∠27° (Fig. 14). Currently, the landslide is basically stable. However, the serious deforming mass shows poor stability, which is more likely to generate a wave by mass sliding into the river.

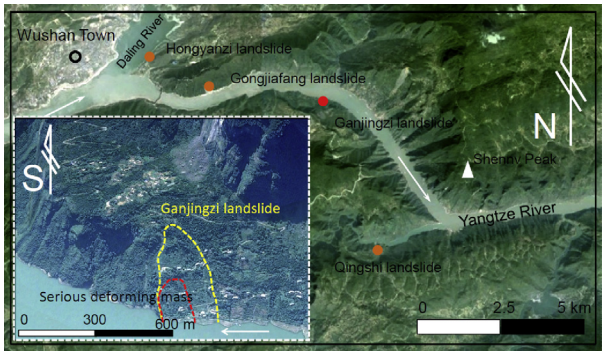

Fig. 13. Location and geomorphologic map of Ganjingzi landslide in Wushan County, Chongqing. The lower left box refers to the geomorphologic map of the Ganjingzi landslide region, and the black big box refers to the numerical calculation range of the landslide-induced impulsive wave.

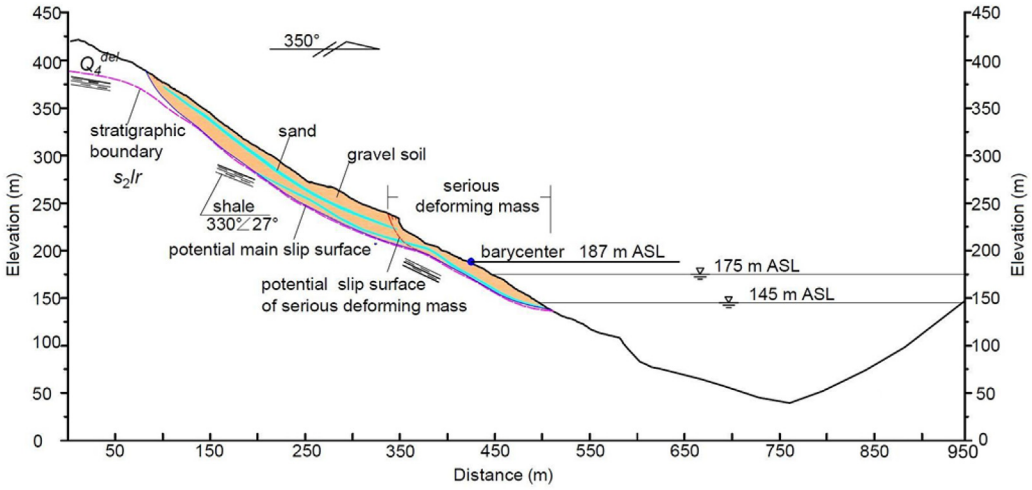

Fig. 14. Engineering geological section of Ganjingzi landslide in Wushan County, Chongqing.

4.2.2. Numerical analysis of landslide-induced impulsive waves

Methods for analysis of landslide-induced impulsive waves include the formula calculation method, physical test method, and numerical method (Fritz, 2002; Pastor et al., 2009; Ataie-Ashtiani and Yavari-Ramshe, 2011; Huang et al., 2012; Wang et al., 2016). With respect to the impulsive wave in the complicated channel area, the numerical method is generally used. According to the mathematical model adopted, the numerical method can be mainly divided into the full Navier–Stokes equation method and the water wave dynamics method. In the case of analyzing fluid-mass-interaction problems in the near field region, the Navier–Stokes equation shows good potential. However, in the case of calculating a wide range channel surge, considerable computing resources are required, which is time-costly. The water wave dynamics method benefits from computation domain, accuracy and speed. In this paper, the open source Geowave code was employed to analyze the landslide-induced impulsive wave. Geowave comprises the tsunami open and progressive initial conditions system (TOPICS) and the FUNWAVE module. The TOPICS makes use of a series of experimental and empirical formulae to produce an initial water wave source field. FUNWAVE is a computation module for wave propagation and run-up based on a nonlinear Boussinesq water wave model. With the help of Geowave, considerable progress on the understanding of impulsive waves has been made (Watts et al., 2003; AFE and CACR, 2008; Tappin et al., 2008; Huang et al., 2012, 2016a).

This text aims to depict the potential impulse wave risk of a single landslide. The landslide kinematic velocity is simply estimated with Newton's laws of motion for a mass point. Assuming that the landslide mass maintains constant acceleration and deceleration motion, Newton's laws show that the maximum moving speed of a mass point on the landslide can be calculated given the known sliding distance and acceleration. Fig. 14 shows that the barycenter elevation of the serious deforming mass is 187 m ASL. On the basis of the isovolumetric method, it is assumed that the serious deforming mass rushes into the water completely and reaches the river bottom after sliding. The sliding distance above the water body under 175 m ASL is 26 m, and the sliding distance above the water body under 145 m ASL is 47 m. Since the material composition and landform of the Ganjingzi landslide are very similar to those of the Xintan landslide (Chen et al., 1985), relevant motion parameters of serious deforming mass of the Xintan landslide can be used. A previous study showed that the maximum acceleration of the Xintan landslide was 2.5 m/s^2, and the maximum underwater deceleration was −1.7 m/s^2 (Wang and Yin, 2003). Then, the maximum speed and underwater movement of the serious deforming mass of Ganjingzi landslide under various water levels can be estimated by Newton's laws of motion. Under the water level at 175 m ASL, the potential maximum speed in the strong deformation region is 8.1 m/s. Underwater movement distance and time are about 40 m and 9.5 s, respectively, and the water depth of the mass stop position is 20 m. Under the water level at 145 m ASL, the potential maximum speed in the strong deformation region is 10.8 m/s. Underwater movement distance and time are about 68 m and 13 s, respectively, and the water depth of the mass stop position is 34 m.

The computation domain of the channel refers to the main channel section of the Yangtze River from Wushan County to Baolong, including Daning River, Hengshixi, Goddess Stream, Baolong Stream. The area is mainly composed of the Yangtze River gorge geomorphologic region. In the computation domain, the east-to-west and south-to-north lengths are about 18 km and 10.4 km, respectively. The computation domain is divided into 750 columns and 435 lines by a grid of 24 m × 24 m. The simulation includes two water level conditions, i.e. 175 m and 145 m ASL. Since the other water levels are between 175 m and 145 m ASL, their wave scales can be linearly included. Therefore, using these two working conditions, the general information of the surge produced by the serious deforming mass of Ganjingzi landslide can be predicted. Table 6 provides the input parameters under two working conditions.

The calculation results show that the maximum impulsive wave amplitude (22 m) under 175 m ASL is slightly higher than that (17.2 m) under the 145 m ASL water level. Under the water level at 175 m ASL, numerical results indicate that after the landslide mass completely rushes into the water, the maximum impulse wave (amplitude of 22 m) will occur at $T = 12.2$ s; the wave will strike the opposite bank at $T = 25.8$ s, and the maximum run-up on the opposite bank will be 10 m high. Thereafter, the impulsive wave will propagate in a direction along the river channel rather than in a radial direction. When $T = 442$ s, the impulsive wave will propagate to Gongjiafang, and the maximum wave will be about 1.39 m high. When $T = 624$ s, the wave will propagate to Jianchuandong, and the maximum wave will be about 0.5 m high. When $T = 852$ s, the maximum surge will propagate to Wushan wharf, and the maximum run-up will be about 0.37 m high. When $T = 1120$ s, the wave of the surge source will be 1 m high, and there will still be waves with a height over 1 m in a few positions. Fig. 15 shows the

Table 6
Input parameters of landslide-induced surge source.

Working condition	Landslide volume (10^4 m^3)	Landslide width (m)	Water depth of barycenter where landslide stops (m)	Maximum sliding speed (m/s)	Underwater sliding distance (m)	Underwater sliding time (s)	Sliding direction (°)
175 m ASL	20	100	20	8.1	40	9.5	351
145 m ASL	20	100	34	10.8	68	13	351

distribution of the maximum impulsive wave amplitude in the channel under 175 m and 145 m ASL. It can be seen from this figure that the impulsive wave decays sharply in the vicinity of the region where the mass slides into the water, but it decays slowly in the peripheral channel.

Based on the impulsive wave simulations under two working conditions, the early-warning region related to the shipping risk could be classified. The scope of the red warning region with waves over 3 m high includes 650 m upstream and 380 m downstream of the Ganjingzi landslide, resulting in a 1030 m long main channel. In the gully upstream and downstream where the landform is narrow, there is some local red warning regions resulting from the wave magnification effect. The orange warning region of wave height of 2–3 m is mainly distributed in the peripheral area of the red warning region, i.e. areas 720 m and 200 m long in the upstream and downstream regions, respectively. The yellow warning region of wave height of 1–2 m is distributed in the peripheral area of the orange warning region, i.e. areas 700 m and 600 m long in the upstream and downstream regions, respectively. These regions are distributed in a concave position in the middle and extend to both wings along the bank slope.

The red and orange warning regions of the potential water wave include four freight and passenger dock terminals, one small diversion-type hydropower station and a main channel nearly 2 km long. As the water wave risk of Ganjingzi landslide is high, emergency prevention preparations began on this landslide in 2016.

4.2.3. *Evaluation of potential impulsive wave risk in TGR*

An impulsive wave generated by a single landslide may endanger the safety of shipping and riparian facilities within several kilometers. In the TGR region, there are numerous landslide collapses, covering an extensive range of channels and riversides. Therefore, identification of landslides with a potential impulsive wave risk in the TGR should be improved.

According to the global landslide-induced impulsive wave cases and the results (Fritz, 2002), a disastrous wave could be formed by rock/soil mass with a certain volume rushing into the water body at a certain speed. A large-scale surge disaster will not be produced by a sliding velocity lower than 1 m/s. According to landslide speed classifications of WP/WLI (1995) and Cruden and Varnes (1996), a movement speed higher than 1 m/s belongs to the category of "very rapid-extremely rapid". Therefore, only mass that moves rapidly can form a large wave, and a landslide with potential rapid movement is the main concern. According to WP/WLI (1995), Cruden and Varnes (1996), Hungr and Evans (2004), and Hungr et al. (2014), rapid movement occurs frequently in plane slide, gravel soil slide, reverse cataclastic rock collapse, and rock fall. Therefore, these types of landslides may be considered as the potential impulsive wave sources in TGR. In this case, a potential landslide-induced impulsive wave risk region in TGR can be roughly identified.

In the lower reservoir section of TGR, i.e. 30 km from the dam, there is no landslide that may generate impulsive wave hazards for the dam. When the landslide is more than 30 km away from the dam, the surge height will be lower than 1 m when it arrives at the dam, and the formed dynamic water pressure will not affect the dam safety; thus, there are no flood hazards that will overtop the dam.

In the bedding bank sections, gorge sections and accumulation or old landslide regions of the middle and upper reservoir sections of the TGR region, a landslide-induced impulsive wave hazard may occur. There are landslide-induced impulsive wave risks in Yunyang-Fengjie region, Diaozui region of Qutang Gorge, Gongjiafang-Dulong region in Wushan County, Qingshi-Peishi region of Wu Gorge, and Huoyanshi region in Badong County. Field

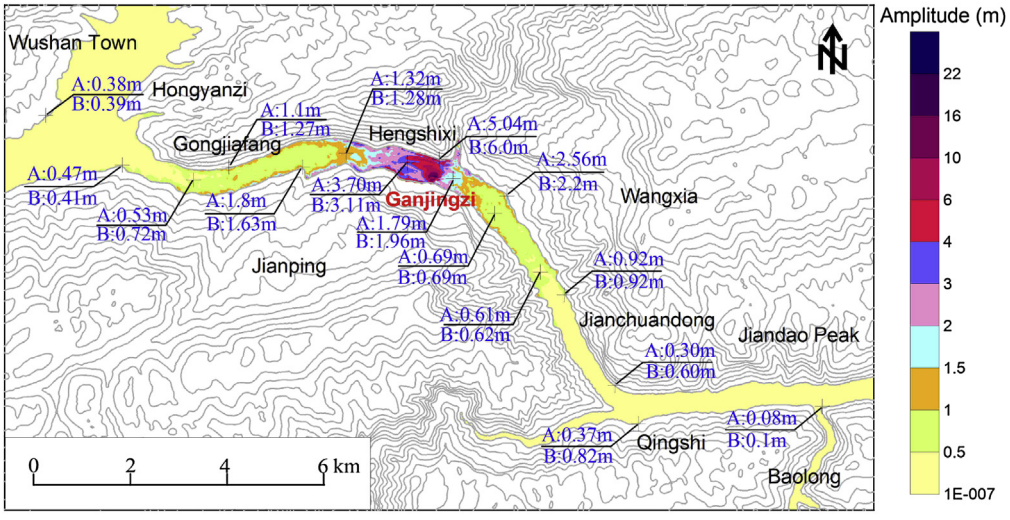

Fig. 15. Distribution map of maximum wave amplitude along the river under two working conditions. The color contour image shows the maximum wave height in the channel under 175 m ASL. At each point, A shows the calculated value under 175 m ASL, and B shows the calculated value under 145 m ASL.

investigation, monitoring and research on the banks of these regions are of priority.

5. Reservoir regulation based on landslide risk control

As a result of the six periods of the 175 m ASL trial impoundment, a large number of reservoir-induced landslides were reported, and some landslides generated impulse wave disasters. The landslides and the triggered impulsive waves caused significant economic losses and casualties. Meanwhile, there is a risk of social-economic losses if navigation is closed due to landslide occurrence. Reservoir-induced landslide occurrence is related to water level regulation. Since the 175 m ASL trial impoundment in 2008, TGR operation has always been conducted using an index of 1-d water level variation. The threshold of the index assumes that the water level drawdown rate does not exceed 0.6 m/d and the rate of the water level increase does not exceed 1 m/d. This assumption was formulated according to reservoir-induced landslide risk control.

However, using the index of the 1-d water level variation is not reasonable for the purpose of reservoir operation regulation and landslide risk control. Firstly, reservoir-induced landslide occurrence relates to the local water level. Generally, there is a lagging period between the local water level and the water level at the front of the dam. Since the reservoir is 600 km long, the water level in areas away from the dam cannot be synchronized in time with respect to impoundment or drawdown at the front of the dam. The water level at the front of the dam on a single day cannot well reflect the local water level in a remote region; thus, the index of several days (such as 5-d or 10-d) water level can generally be used. Secondly, if merely using a single-day index, water resources are not rationally utilized, and a potential flood disaster will occur. Before the arrival of an upstream flood, reservoir water storage cannot be emptied in time due to control of the water level speed, and there is a potential hazard risk of overtopping the dam. Meanwhile, because of the control of the rate at which the water level increases, upstream water cannot be stored in time, which can lead to waste of water resources. Subsequently, impoundment is difficult based on a normal design water level during the flood recession period. Therefore, the 1-d water level variation index will be optimized in the reservoir operation regulation of TGR.

In this paper, 1-d, 5-d and 10-d water level variation indices are adopted, and the relationship between reservoir operation regulation and landslide risk control is analyzed and discussed.

5.1. Relationship between water level variation and landslides after 175 m ASL trial impoundment

According to the temporal distribution characteristics of landslides after the 175 m ASL trial impoundment, there were relatively more landslides and obvious regularity in the first three trials ("initial period"); in the next three trials ("the second period"), landslide occurrences were randomly distributed.

5.1.1. Relationship between water level variation and landslides in initial period

Table 7 shows the maximum ten periods of the 5-d water level increase variation and the corresponding landslide occurrences during the initial period. The landslide occurrences refer to the number of landslides occurring in the previous 5 d and the next 5 d, which aims to consider the lagging period between water level variation and landslide occurrence. The variation in water level increase from 30 October to 4 November 2008 reached 8.32 m, with an average rate of 1.66 m/d. A total of 37 landslides were observed in 10 d, which is the highest landslide occurrence since 2008. Landslides always occur when the daily water level increase rate reaches 1.66–2.25 m/d. It shows that when water level increase variation exceeds 1.66 m/d, the probability of landslide occurrence is very high.

Table 7
Statistics of maximum ten occurrences of 5-d water level variation in initial stage.

Date	5-d increase of water level (m)	Average daily increase of water level (m)	Number of landslides
28 September to 3 October 2008	8.36	1.67	3
21–26 October 2008	3.98	0.77	2
30 October to 4 November 2008	8.32	1.66	37
3–8 August 2009	7.90	1.58	0
14–19 September 2009	5.31	1.06	0
29 September to 4 October 2009	4.12	0.82	2
10–15 July 2010	3.72	0.74	1
18–23 July 2010	11.9	2.38	1
27 July to 1 August 2010	4.09	0.82	2
22–27 August 2010	11.25	2.25	0

Table 8 shows the maximum ten events of the 5-d variation in water level drawdown and the corresponding landslide number during the initial period. The ten events were mainly distributed in the flood season, i.e. the cumulative drawdown from 1 to 6 August 2010, reached 5.57 m. The average rate was 1.15 m/d, which is the maximum average daily drop since 2008. There is no record for landslide occurrence over 10 d. This shows that there is no strong correlation between reservoir water level variation and landslide occurrence.

5.1.2. Relationship between water level variation and landslides in second period

In the latter three trials, there were fewer landslides, suggesting few disasters. The landslide occurrence and associated disasters were in an acceptable range for the Three Gorges Project. Table 9 indicates the indices ranges of several water level variations since 2012, which may be an important reference for the normal operation of TGR in the future.

Meanwhile, further statistics on maximum water level variation indices and the corresponding landslide number in the second period are needed. The five greatest variations in the 1-d increases occurred mainly in September 2011, September 2012, and July 2012, and the highest water level increase reached 3.21 m/d. The five greatest variations in the 1-d drawdowns were mainly distributed in the period of water level regulation for flood prevention (from May to August). The maximum 1-d drawdown reached 2.79 m/d on 1 May 2013. However, no reservoir-induced landslide occurred within these 10 d.

The periods of the great water level variation in the 5-d water level increases were mainly distributed in the flood season, i.e. from July to September. The maximum 5-d water level increase up to

Table 8
Statistics of maximum ten occurrences of 5-d water level drawdown in initial stage.

Date	5-d drawdown of water level (m)	Average daily drawdown of water level (m)	Number of landslides
21–26 May 2009	2.63	0.526	2
31 May to 5 June 2009	2.56	0.512	3
11–16 August 2009	4.07	0.814	1
4–9 June 2010	2.12	0.424	1
28 June to 2 July 2010	3.09	0.618	0
13–18 July 2010	3.14	0.628	2
23–28 July 2010	2.01	0.402	1
1–6 August 2010	5.75	1.15	0
7–12 August 2010	5.38	1.076	0
26–31 May 2011	2.56	0.512	0

Table 9
Water level variation parameters in second stage.

Time (d)	Total variation (m)		Average rate (m/d)		Average rate over several days (m/d)*	
	Rising	Drawdown	Rising	Drawdown	Rising	Drawdown
1	1.2–1.4	0.8–1	1.2–1.4	0.8–1	0.45	0.15
5	5.5–6.5	3.5–4.5	1.1–1.3	0.7–0.9		
10	10–12	6–8	1–1.2	0.6–0.8		

Note: *Average rate over several days refers to the overall process of rising (more than 45 d) and drawdown (more than 160 d) in the 175 m ASL impoundment.

9.44 m occurred during 1–6 September 2012. The periods of the greatest variation in the 5-d water level drawdown were mainly distributed from May to August. The largest variation appeared on 13–18 August 2012, followed by 10–15 August 2013, with drawdown rates of 5.77 m/5 d and 5.45 m/5 d and average daily rates of 1.15 m/d and 1.09 m/d, respectively. However, no reservoir-induced landslide was reported within these 10 d.

The periods of the great variation in the 10-d water level increase were also mainly distributed from July to September. The maximum value of 13.87 m occurred during 14–24 September 2011, with an average rate of 1.39 m/d. The periods of greatest variation in the 10-d water level drawdown were mainly distributed from May to August. The maximum value of 10.65 m occurred during 12–22 August 2012, with an average drawdown rate of 1.07 m/d. Similarly, no reservoir-induced landslide occurred within these 10 d.

During three periods of the 175 m ASL trials since 2011, reservoir-induced landslides significantly decreased, and only a few were reported. However, the landslides appeared to have excessive deformations, such as the Bazimen, Baijiabao, Baishuihe, and Songjiawuchang landslides in Hubei Province, and the Dingjiawan, Zhangjiawan, Laoyingbei, Fengjiawan, and Sanzhouxi landslides in Chongqing. The water level drawdown rate increased from mid-May to early June, 2012. During June 5–10, the reservoir 5-d water level drawdown rate reached 3.99 m/5 d, with a maximum of 1.01 m/d and an average of 0.8 m/d. The daily deformation rate measured in Shuping landslide reached 1.4–3.6 cm/d. This indicates that rapid water level variation has a significant influence on landslide instability.

5.2. Influence of water level variation rate on a typical landslide

Taking Shuping landslide for example, the reservoir water level varies between 145 m and 175 m, and computing periods are 30 d and 180 d. The water level change rates are set as ±0.2, ±0.4, ±0.6, ±0.8, ±1, ±1.2, ±1.4, ±1.6, ±1.8 and ±2 m/d. In the computation, the Janbu limit equilibrium method coupled with transient seepage analysis was adopted to calculate the variation in FOS of the landslide. Figs. 16 and 17 indicate the FOS time-history curves of the landslide when the reservoir water level ranged between 145 m and 175 m.

In Fig. 16, it can be seen that the FOS of the landslide increases with the reservoir water level increase during the initial impoundment period. The groundwater level increase within the landslide mass lags behind the reservoir water level. As a result, the stabilizing effect can be formed by the pressure difference between the lower internal pressure and higher external pressure of the landslide, which is helpful for landslide stability. When the reservoir water level is stable, i.e. water level of 175 m ASL, the groundwater level within the mass will also gradually increase with elapsed time. The pressure difference inside and outside the landslide will dissipate gradually, leading to a decrease in FOS. Such a dissipation process is related to the permeability of the mass. The final FOS will be lower than the original FOS when a high water level is maintained.

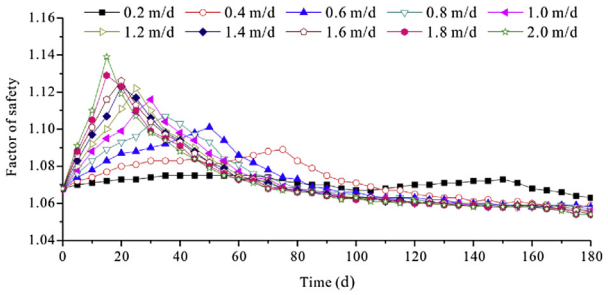

Fig. 16. FOS variation of Shuping landslide under various water level increasing rates.

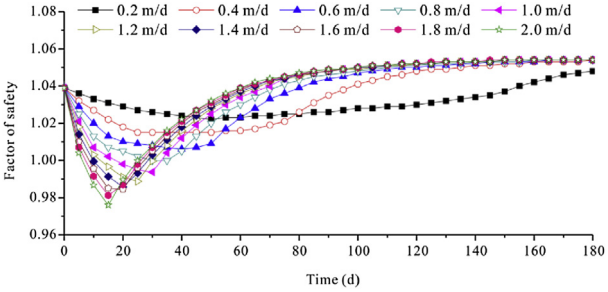

Fig. 17. FOS variation of Shuping landslide under various water level drawdown rates.

When the reservoir water level decreases from 175 m to 145 m ASL, the FOS of the landslide exhibits an initial downward trend (Fig. 17). The groundwater level decrease within the mass lags behind the reservoir water level. As a result, the pressure difference formed between the higher internal pressure and lower external pressure makes the landslide more unstable (Jiang et al., 2011; Pinyol et al., 2012). A faster drawdown rate of the reservoir water level will lead to a faster decrease in FOS. As a result, when the water level drawdown rate is around 1 m/d, the minimum FOS is 0.99–1.01, and the landslide is in a limited equilibrium state. When the water level drawdown rate exceeds 1.4 m/d, the minimum FOS is less than 0.9. When the reservoir water level is maintained at 145 m ASL, the groundwater level will also gradually decrease to a stable water level with elapsed time. The pressure difference inside and outside the landslide will be reduced gradually, which leads to an increase in FOS of landslide.

According to the analysis of the influence of different water level variation rates on the stability of the Shuping landslide, it can be seen that the water level variation rate has a strong influence on landslide stability. Predictably, different permeable masses will have different influences on landslide stability at different water level variation rates. However, a high water level variation rate (e.g. a drawdown daily rate greater than 1 m/d) will definitely have a strong impact on landslide stability.

5.3. Water level variation ranges based on landslide risk control

5.3.1. Suggestions for water level variation ranges

In the period of the first 175 m ASL trial impoundment and drawdown, many landslides were induced and were associated with huge losses, which resulted in social pressure on the Three Gorges Project. The landslide risk in this period can be considered to be unacceptable. After the first trial, the number of landslides induced by the reservoir declined sharply. Only 25 landslides were reported in the latter five periods of the 175 m ASL impoundment.

The landslides were randomly distributed, which suggests that landslides in TGR are controllable, and the risk is acceptable in a global sense. The criteria can be established herein: (i) if the annual landslide number $N \geq 100$, the risk of a landslide being caused by water level variation in TGR is unacceptable; (ii) if $N < 25$, the risk is acceptable; and (iii) when $100 > N \geq 25$, the landslide risk is as low as reasonably practical (ALARP). It is noted that the acceptability level of the number of reservoir-induced landslides is not identical to the acceptability degree of landslide hazards. For example, the considerable risk of a landslide-induced wave, such as Vajont landslide, is unacceptable. In this case, the reservoir regulation should be controlled according to the risk of the landslide and the landslide-induced wave.

According to the statistical analysis of the 5-d water level increase and the number of landslides listed in Table 7, it can be seen that there is no clear correlation between these factors (Fig. 18). According to Table 8, it can be seen that the correlation between them is low. Pure mathematical statistics for other water level variation indices also show similar results. Therefore, it is difficult to obtain a threshold value of water level variation indices that is fully dependent on mathematical statistics.

Using statistical analysis, the calculated FOS of a typical landslide and experienced judgment, a proposal (Table 10) for 1-d, 5-d and 10-d water level variation indices is suggested in terms of landslide risk control. The three indices in Table 10 belong to a union of sets. If one water level variation value exceeds a higher threshold index, it will reach the corresponding risk degree. In specific implementation, it will be operated according to the water level variation indices for acceptable risk. For example, when the maximum daily increase in the water level is less than 1.17 m, or the maximum daily drawdown water level is less than 0.83 m, it could be expected that the number of annual landslides will be less than 25 (see Table 11).

5.3.2. Validation from the 7th 175 m ASL trial impoundment

Table 10 is proposed based on the six periods of the 175 m ASL trial impoundment. To validate the rationality and reliability of established indices, data from September 2014 to August 2015 (the 7th 175 m ASL trial impoundment) were analyzed in this study.

In early June 2015, the water level in TGR decreased from 154 m to 145.1 m ASL. Fig. 19 shows the 1-d, 5-d, and 10-d curves for water level variations in June 2015. Three periods of 1-d water level drawdown were observed, which were 0.91 m on June 14, 0.99 m on June 19, and 1.07 m on June 21. According to the threshold values in Table 10, they are within the unacceptable risk threshold range. In that period, four landslides occurred in the TGR region, which were Zhujiadian landslide in Badong County (on 26 June 2016, with a mass volume of about 1.43×10^6 m^3), Ganjingzi landslide in Wushan County (on 16 June 2016, with a volume of about 2×10^6 m^3), Hongyanzi landslide in Wushan County (on 24 June 2016, with a volume of about 0.2×10^6 m^3) and Huangjuebang landslide in Fuling District (on 15 June 2016, with a volume of about 0.66×10^6 m^3). In 2015, 12 reservoir-induced landslides were reported in the TGR, and four landslides accounted for 1/3 of the total.

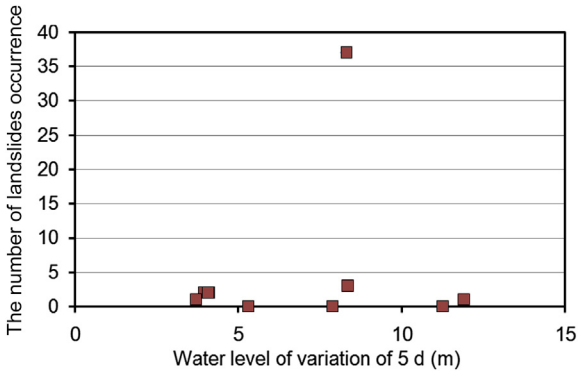

Fig. 18. Scatter diagram showing landslide number and 5-d water level variation.

On 21 June 2015, a severe deformation occurred in the toe of Hongyanzi landslide in Wushan County on the left bank entrance to Daning River, a tributary of the Yangtze River. On June 24, the landslide failed; 0.2×10^6 m^3 soil mass rushed into the reservoir, and Wushan New County on the opposite bank was struck by the induced water wave. As a result, two people were killed, four people were injured, and 13 boats capsized. It seems that there is an evident correlation between the Hongyanzi landslide and the water level drawdown (Huang et al., 2016a). On 16 June 2015, a serious deformation appeared in the toe of Ganjingzi landslide of Wushan County, and the deformation continued for nearly 15 d. Because the potential water wave risk was predicted prior to the Ganjingzi landslide occurrence, navigation in the Wu Gorge section of the Yangtze River was closed on June 27. This indicates that Table 10 has good reliability, and can be used as reference for water level regulation in TGR.

6. Discussion

It can be seen from the deformation curves of Shuping and Outang landslides that the deformation for both landslides shows nearly linear growth, the only difference is the triggering factor of deformation acceleration. As a result, occurrence of reservoir-induced landslides will be affected by reservoir regulation, but it is not the only factor for many reservoir-induced landslides.

The relationship between water level variation indices and landslide occurrence suggests the establishment of water level variation threshold values based on statistics of local water level variation for each landslide occurrence. Alternatively, the mechanism category of each landslide could be used. However, due to the oversized investigation area and data shortage, such work is very difficult at present.

In Table 11, 13 large-scale landslides subjected to global sliding or local sliding in the 175 m ASL trial impoundment were further used, and water level variations were analyzed. It can be seen that there is no obvious correlation between the water level variation range and the time of landslide occurrence. Many landslides occur at low water level variations (see Fig. 20). This indicates the complexity and diversity of the reservoir-induced landslide occurrence mechanism (Wang et al., 2008a; Zhang et al., 2010; Xia et al., 2013; Lu, 2015).

Since the 175 m ASL trial impoundment in September 2008, landslides mainly occurred during the initial stage of water level increase. In the second stage, landslides mainly occurred during the water level drawdown periods. In recent years, the time of landslide occurrence gradually changed to the flood season, which was induced mainly by the coupled effects of water level variation and rainstorms. This also shows that the influence of reservoir water variation on landslides does not reveal strict periodicity. In fact, since the slope mass in the water level variation zone is subjected to long-term scouring, undercutting and periodic immersion-exposure, structural damage, and rock/soil property deterioration at the water level of 145–175 m ASL may lead to the occurrence of new landslides in the future (Mazaeva et al., 2013; Huang et al., 2016b).

7. Conclusions

This paper first describes the spatiotemporal distribution patterns of landslide occurrences during the six periods of the 175 m

Table 10
Suggestions for various water level variation indices.

Risk degree	Value type	1-d water level variation (m)				5-d water level variation (m)				10-d water level variation (m)			
		Rising		Drawdown		Rising		Drawdown		Rising		Drawdown	
		Minimum	Maximum	Minimum	Maximum	Minimum	Maximum	Minimum	Maximum	Minimum	Maximum	Minimum	Maximum
Acceptable	Total	1–1.17		0.67	0.83	3.6	4.38	2.92	3.75	8.33	10	5	6.67
	Average	0.83	1.17	0.67	0.83	0.72	0.88	0.58	0.75	0.83	1	0.5	0.67
ALARP	Total	1.17	1.27	0.73	0.91	4.38	6	3.75	4.09	10	10.91	6.67	7.27
	Average	1.17	1.27	0.73	0.91	0.88	1.2	0.75	0.82	1	1.09	0.67	0.73
Unacceptable	Total	1.27	1.4	0.91	1	6	6.5	4.09	4.5	10.91	12	7.27	8
	Average	1.27	1.4	0.91	1	1.2	1.3	0.82	0.9	1.09	1.2	0.73	0.8

Table 11
Occurrence date and current maximum water level variation of 13 typical reservoir-induced landslides.

No.	Landslide name	Volume (10^4 m^3)	Sliding scale	Occurrence date (yy/mm/dd)	Water level variation (m)*		
					1-d	5-d	10-d
1	Zengjiapeng landslide	487	Global	2012/5/31	−0.5	−3.1	−4.9
2	Huanglianshu landslide	515	Global	2012/5/31	−0.5	−3.1	−4.9
3	Hongyanzi landslide	20	Global	2015/6/24	−1.1	−4	−7.1
4	Fengbaoling landslide	15.4	Local	2010/3/1	−0.3	−1.3	−2.4
5	Changzheng landslide	435	Local	2008/11/9	2	8.3	11.3
6	Tugouzidong landslide	286	Global	2008/11/6	2	8.3	11.3
7	Tangjiao landslide	102	Local	2007/4/1	−0.1	0.5	0.9
8	Gongjiafang landslide	38	Global	2008/11/23	−0.2	−0.8	4.6
9	Lijiapo landslide	25	Local	2008/11/2	2	5.8	9.2
10	Qingshi landslide	1500	Local	2010/10/26	0.5	3.4	6.5
11	Chuanzhu landslide	100	Global	2008/11/22	−0.2	−0.8	11.3
12	Liangshuijing landslide	360	Local	2008/11/22	−0.2	−0.8	11.3
13	Nierwang landslide	80	Global	2008/11/5	2	8.3	11.3

Note: *Positive value refers to water level increase, and negative value refers to water level drawdown.

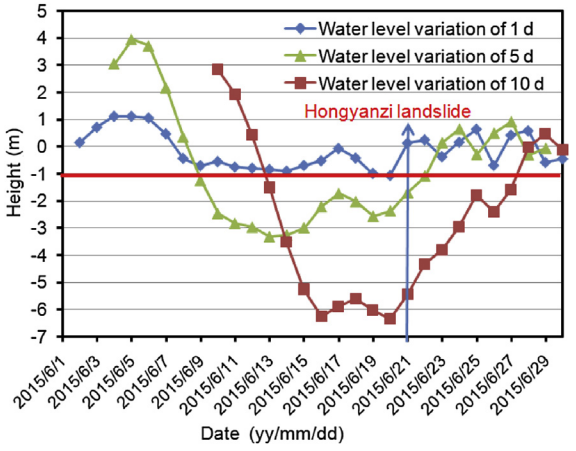

Fig. 19. Relationship between water level variations of TGR and landslide risk threshold in June 2015. The red straight line refers to the unacceptable threshold value of the 1-d water level variation index, which was broken on 20 June 2015.

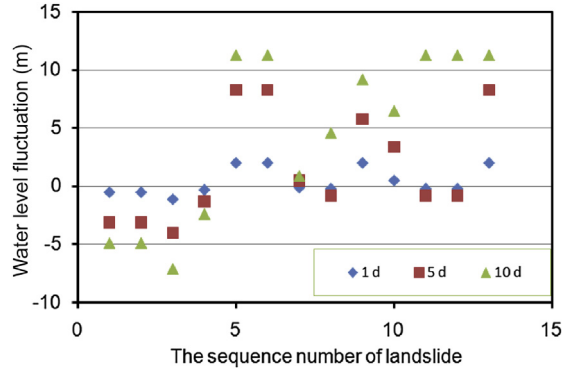

Fig. 20. Scatter diagram of water level fluctuations of 13 typical landslides before failure.

ASL trial impoundment from 2008 to 2014. The number of landslides decreased from 273 during the initial stage to less than 10 during the second stage. The geological disasters caused by the reservoir changed from a high-risk level to a low-risk level. The landslides caused by the 175 m ASL trial impoundment in TGR mainly consisted of accumulation landslides and dip-slope landslides, and old landslide reactivation accounted for about 66.8% of the reservoir-induced landslides. Focusing on Shuping accumulation landslides and the Outang dip-slope landslide, two types of old landslide reactivation mechanisms are analyzed. The results show that the reactivation triggering factor of accumulation landslides is mainly related to the water level variation, and reactivation triggering factors of dip-slope landslides are related to water level variation and precipitation.

After impoundment in the TGR, the landslide-induced surge hazard risk increases significantly, which threatens the safety of the channel and riparian towns. Taking the Ganjingzi landslide in Wushan County for example, the potential zone of impulsive wave hazards of an individual landslide could be more than 2 km long. Suggestions for 1-d, 5-d, and 10-d water level variation indices are proposed. When the maximum 1-d water level increase is less than 1.17 m, or the maximum 1-d water level drawdown is less than 0.83 m, it could be expected that the number of annual landslides will be less than 25. In addition, the rationality and reliability of the proposed indices are verified, which is helpful for landslide risk control in the TGR.

Conflict of interest

We wish to confirm that there are no known conflicts of interest associated with this publication and there has been no significant financial support for this work that could have influenced its outcome.

Acknowledgments

The “Twelfth Five-Year Plan” of the National Science and Technology Support Project (Grant No. 2012BAK10B01), the National Natural Science Foundation of China (Grant Nos. 41372321 and 41502305) and China Geological Survey Projects (Grant No. 121201009000150018) are appreciated. Special thanks are given to Profs. Sijing Wang, Yaoru Lu, Zuyu Chen, Qihu Qian, and Houqun Chen.

References

Applied Fluids Engineering, Inc. (AFE), Center for Applied Coastal Research (CACR). Geowave 1.1 tutorial. Newark: University of Delaware; 2008.
Ataie-Ashtiani B, Yavari-Ramshe S. Numerical simulation of wave generated by landslide incidents in dam reservoirs. Landslides 2011;8(4):417–32.
Basu D, Green S, Das K, Janetzke R, Stamatakos J. Numerical simulation of surface waves generated by a sub-aerial landslide at Lituya Bay, Alaska. In: Proceedings of OMAE 2009, 28th International Conference on Ocean, Offshore and Arctic Engineering; 2009. p. 1–14.
Berilgen MM. Investigation of stability of slopes under drawdown conditions. Computers and Geotechincs 2007;34(2):81–91.
Bosa S, Petti M. Shallow water numerical model of the wave generated by the Vajont landslide. Environmental Modelling & Software 2013;26(4):406–18.
Breth H. The dynamic of a landslide produced by filling a reservoir. In: Proceedings of the 9th International Congress on Large Dams, Istanbul; 1967. p. 37–45.
Chen DJ, Yang TM, Xue GF, Ren J. Preliminary survey for Jiangjiapo-Xintan landslide in Xiling Gorge of the Yangtze River. Hydroelectricity 1985;10:16–22 (in Chinese).
Chen XT, Huang RQ. Stability analysis of Baijiabao Landslide in Xiangxi River Valley, Hubei Province. Chinese Journal of Geological Hazard and Control 2006;17(4):29–33 (in Chinese).
Chen ZS, Zhang XG. A hazard-chain of landslide-collapse-debris flow-river stoppage in Wulong County, Sichuan Province on April 30, 1994. Mountain Research 1994;12(4):225–9 (in Chinese).
Chen ZY, Morgenstern NR. Extensions to the generalized method of slices for stability analysis. Canadian Geotechnical Journal 1983;20(1):104–19.
Chengdu College of Geology. Research on formation mechanism and stability of rainstorm landslide in Sichuan Basin. Research report for slope stability in Southwest mountainous area subject to collapse disasters. Chengdu: Chengdu College of Geology; 1986 (in Chinese).
Collins BD, Znidarcic D. Stability analyses of rainfall induced landslides. Journal of Geotechnical and Geoenvironmental Engineering 2004;130(4):362–72.
Crosta GB, Frattini P. Rainfall-induced landslides and debris flows. Hydrological Processes 2008;22(4):473–7.
Cruden DM, Varnes DJ. Landslide types and processes. In: Landslides: Investigation and mitigation. Special report 247. Washington, D.C.: Transportation Research Board, US National Research Council; 1996. p. 36–75.
Duncan J, Wrigth S, Wong K. Slope stability during rapid drawdown. In: Proceedings of the H. Bolton Seed Memorial Symposium; 1990. p. 253–72.
Fredlund DG, Rahardjo H. Soil mechanics for unsaturated soils [Chen ZY, Zhang ZM, Chen YJ, Trans.]. Beijing: China Architecture and Building Press; 1997 (in Chinese).
Fritz HM. Initial phase of landslide generated impulse waves. PhD Thesis. Zürich: ETH. 2002.
Geo-Slope International, Ltd. Stability modeling with SEEP/W 2007-An engineering methodology. Calgary, Alberta: Geo-Slope International, Ltd.; 2008a.
Geo-Slope International, Ltd. Stability modeling with Slope/W 2007-An engineering methodology. Calgary, Alberta: Geo-Slope International, Ltd.; 2008b.
Ghimire M. Landslide occurrence and its relation with terrain factors in the Siwalik Hills, Nepal: case study of susceptibility assessment in three basins. Natural Hazards 2011;56(1):299–320.
Guo J, Xu M, Zhao Y. Study on reactivation and deformation process of Xierguazi ancient-landslide in Heishui reservoir of southwestern China. In: Engineering Geology for Society and Territory. Springer; 2015. p. 1135–41.
Highland LM, Bobrowsky P. The landslide handbook: a guide to understanding landslides. Circular 1325. Reston, Virginia: U.S. Geological Survey; 2008.
Hu XL, Zhang M, Sun MJ, Huang KX, Song YJ. Deformation characteristics and failure mode of the Zhujiadian landslide in the Three Gorges Reservoir, China. Bulletin of Engineering Geology and the Environment 2015;74(1):1–12.
Huang BL, Chen XT. Deformation and failure mechanism of Baijiabao landslide in Xiangxi River Valley. Chinese Journal of Geotechnical Engineering 2007;29(6):938–42 (in Chinese).
Huang BL, Yin YP, Liu GN, Wang SC, Chen XT, Huo ZT. Analysis of waves generated by Gongjiafang landslide in Wu Gorge, Three Gorges Reservoir, on November 23, 2008. Landslides 2012;9(3):395–405.
Huang BL, Yin YP, Wang SC, Chen XT, Liu GL, Jiang ZB, Liu JZ. A physical similarity model of an impulsive wave generated by Gongjiafang landslide in Three Gorges Reservoir, China. Landslides 2014;11(3):513–25.
Huang BL, Yin YP, Du CL. Risk management study on impulse waves generated by Hongyanzi landslide in Three Gorges Reservoir of China on June 24, 2015. Landslides 2016a;13(3):603–16.
Huang BL, Zhang ZH, Yin YP, Ma F. A case study of pillar-shaped rock mass failure in the Three Gorges Reservoir Area, China. Quarterly Journal of Engineering Geology and Hydrogeology 2016. http://dx.doi.org/10.1144/qjegh2015-034.
Huang BL. Study of impulsive wave generated by landslide in reservoir using water wave dynamic method. PhD Thesis. Wuhan: China University of Geosciences; 2014 (in Chinese).
Hungr O, Evans SG. The occurrence and classification of massive rock slope failure. Felsbau 2004;22:16–23.
Hungr O, Leroueil S, Picarelli L. The Varnes classification of landslide types, an update. Landslides 2014;11(2):167–94.
International Commission on Large Dams (ICOLD). Reservoir landslides: investigation and management. Paris: ICOLD; 2002.
International Geotechnical Society’s UNESCO Working Party on World Landslide Inventory (WP/WLI). A suggested method for describing the rate of movement of a landslide. Bulletin of International Association of Engineering Geology 1995;52:75–8.
Jiang JW, Ehret D, Xiang W, Rohn J, Huang L, Yan SJ, Bi RN. Numerical simulation of Qiaotou Landslide deformation caused by drawdown of the Three Gorges Reservoir, China. Environmental Earth Sciences 2011;62(2):411–9.
Kim TH, Cruden DM, Martin CD, Froese CR. The 2007 Fox Creek landslide, Peace River Lowland, Alberta, Canada. Landslides 2010;7(1):89–98.
Lai Y, Fang J, Zhu TY, Chen KH. The Wushan Qingshi Landslide resurrection mechanism and stability evaluation. Chinese Journal of Underground Space and Engineering 2015;11(4):1039–46 (in Chinese).
Lane PA, Griffiths DV. Assessment of stability of slopes under drawdown conditions. Journal of Geotechnical and Geoenvironmental Engineering 2000;126(5):443–50.
Li DY, Yin KL, Leo C. Analysis of Baishuihe landslide influenced by the effects of reservoir water and rainfall. Environmental Earth Sciences 2010;60(4):677–87.
Li SD, Li X, Wu J, Liu YH. Evolution process and pattern of sliding zone in large consequent bedding rock landslide. Chinese Journal of Rock Mechanics and Engineering 2007;26(12):2473–80 (in Chinese).
Li YS. Character and stability analysis for Jipazi landslide. Hydrogeology and Engineering Geology 1984;6:5–10 (in Chinese).
Liu GR, Chu ZC, Guo XZ, Liu Y. Summary of main achievements of important geological and seismological problems in Three Gorges of Yangtze River. Chinese Journal of Geological Hazard and Control 1992;3(1):7–14 (in Chinese).

Liu GY. Influence of water table fluctuation on stability of colluvial landslide in Three Gorges Reservoir. Safety and Environmental Engineering 2011;18(5):26–8 (in Chinese).
Liu SK. The decay study on the impulse wave generated by Xintan landslide of Xiling Gorges, the Yangtze River. Water Resources and Hydropower Engineering 1987;(9):11–4 (in Chinese).
Lu SS. Study on the bedding rock landslide development rule and failure mechanism in Three Gorges Reservoir area. MS Thesis. Xianyang: Northwest A & F University; 2011 (in Chinese).
Lu YF. Deformation and failure mechanism of slope in three dimensions. Journal of Rock Mechanics and Geotechnical Engineering 2015;7(2):109–19.
Mazaeva O, Khakand V, Kozyreva E. Model of erosion-landslide interaction in the context of the reservoir water level variations (East Siberia, Russia): factors, environment and mechanisms. Journal of Earth System Science 2013;122(6):1515–31.
Morgenstern NR, Price V. The analysis of the stability of general slip surface. Géotechnique 1965;15(l):79–93.
Müller L. The rock slide in the Vajont Valley. Rock Mechanics and Engineering Geology 1964;(2):148–212.
Pastor M, Herreros I, Fernández Merodo JA, Mira P, Haddad B, Quecedo M, González E, Alvarez-Cedrón C, Drempetic V. Modelling of fast catastrophic landslides and impulse waves induced by them in fjords, lakes and reservoirs. Engineering Geology 2009;109(1–2):124–34.
Pinyol NM, Alonso EE, Corominas J, Moya J. Canelles landslide: modelling rapid drawdown and fast potential sliding. Landslides 2012;9(1):33–51.
Prokešová R, Medveďová A, Tábořík P, Snopková Z. Towards hydrological triggering mechanisms of large deep-seated landslides. Landslides 2013;10(3):239–54.
Riemer W. Landslides and reservoirs. In: Proceedings of the 6th International Symposium on Landslides. Rotterdam: A.A. Balkema; 1992.
Rodríguez-Peces MJ, Azañón JM, García-Mayordomo J, Yesares J, Troncoso E, Tsige M. The Diezma landslide (A-92 motorway, Southern Spain): history and potential for future reactivation. Bulletin of Engineering Geology and the Environment 2011;70(4):681–9.
Santangelo M, Marchesini I, Cardinali M, Fiorucci F, Rossi M, Bucci F, Guzzetti F. A method for the assessment of the influence of bedding on landslide abundance and types. Landslides 2015;12(2):295–309.
Schuster RL. Reservoir-induced landslides. Bulletin of the International Association of Engineering Geology 1979;20(1):8–15.
Tan L. Stability variation characteristics of Liangshuijing landslide during the Three Gorges Reservoir running. Chinese Journal of Chongqing Jiaotong University: Natural Science 2011;30(Suppl. 1):624–9 (in Chinese).
Tang HM, Li CD, Hu XL, Wang LQ, Criss R, Su AJ, Wu YP, Xiong CR. Deformation response of Huangtupo landslide to rainfall and the changing levels of the Three Gorges Reservoir. Bulletin of Engineering Geology and the Environment 2015;74(3):933–42.
Tang XS, Zhen YR, Tan WP. Evolutionary change mechanism of landslide deformation and failure of accumulative formation in Three Gorges Reservoir. Chongqing Architecture 2012;11(9):10–4 (in Chinese).
Tappin DR, Watts P, Grilli ST. The Papua New Guinea tsunami of 17 July 1998: anatomy of a catastrophic event. Natural Hazards and Earth System Sciences 2008;8(2):243–66.
Terzaghi K. Theoretical soil mechanics. New York: John Wiley and Sons, Inc.; 1944.
Tian ZG, Lu SQ. Analysis of formation mechanism and stability evaluation of Nierwan landslide in the Three Gorges Reservoir area. Resources Environment and Engineering 2012;26(3):236–9 (in Chinese).
Trzhtsinskii YB. Landslides along the Angara reservoirs. Bulletin of the International Association of Engineering Geology 1978;17(1):42–3.
Wang FW, Zhang YM, Huo ZT, Peng XM, Wang SM, Yamasaki S. Mechanism for the rapid motion of the Qianjiangping landslide during reactivation by the first impoundment of the Three Gorges Dam reservoir, China. Landslides 2008a;5(4):379–86.
Wang FW, Zhang YM, Huo ZT, Peng XM, Kiminori A, Wang GH. Movement of the Shuping landslide in the first four years after the initial impoundment of the Three Gorges Dam Reservoir, China. Landslides 2008b;5(3):321–9.
Wang W, Chen GQ, Yin KL, Wang Y, Zhou SH, Liu YL. Modeling of landslide generated impulsive waves considering complex topography in reservoir area. Environmental Earth Sciences 2016;75:372.
Wang Y, Yin KL. Analysis of movement process of landslide in reservoir and calculation of its initial surge height. Earth Science – Journal of China University of Geosciences 2003;28(5):579–82 (in Chinese).
Watts P, Grilli ST, Kirby JT, Fryer GJ, Tappin DR. Landslide tsunami case studies using a Boussinesq model and a fully nonlinear tsunami generation model. Natural Hazards and Earth System Science 2003;3(5):391–402.
Xia M, Ren GM, Ma XL. Deformation and mechanism of landslide influenced by the effects of reservoir water and rainfall, Three Gorges, China. Natural Hazards 2013;68(2):467–82.
Xiao SR, Hu ZY, Lu SS, Ming CT, Chen DQ. Classification of reservoir-triggered landslides in Three Gorges Reservoir area. Chinese Journal of the Yangtze River Scientific Research Institute 2013;30(11):39–44 (in Chinese).
Xin LX. The mechanism and forecasting study on typical accumulation landslide of Three Gorges Reservoir. MS Thesis. Wuhan: China University of Geosciences; 2012 (in Chinese).
Yang H, Chen XY, Zeng FQ. Application and analysis of deformation monitoring technology in Yemaomian landslide. Bulletin of Surveying and Mapping 2012;(6):54–7 (in Chinese).
Yang PB, Lai JF, Chen XY. Application of measurement robot in Yemaomian landslide deformation monitoring. Shanxi Architecture 2008;34(1):352–3 (in Chinese).
Yin YP, Huang BL, Chen XT, Liu GN, Wang SC. Numerical analysis of wave generated by the Qianjiangping landslide in Three Gorges Reservoir, China. Landslides 2015;12(2):355–64.
Yin YP. Human-cutting slope structure and failure pattern at the Three Gorges Reservoir. Journal of Engineering Geology 2005;13(2):145–54 (in Chinese).
Zhang TT, Yan EC, Cheng JT, Zheng Y. Mechanism of reservoir water in the deformation of Hefeng landslide. Journal of Earth Science 2010;21(6):870–5.
Zhao Y, Xu M, Guo J, Zhang Q, Zhao HM, Kang XB, Xia Q. Accumulation characteristics, mechanism, and identification of an ancient translational landslide in China. Landslides 2015;12(6):1119–30.

Yueping Yin received his PhD in Geological Engineering from Chinese Academy of Geological Sciences. He is currently working as chief-geologist at China Institute of Geo-Environment Monitoring, China Geological Survey. Dr. Yin has been conducting researches on landslide prevention at the Three Gorges since 1986, covering relocation siting, monitoring and warning, stabilization, and risk controlling. He is the President of International Consortium of Landslides and the Chairman of Expert Committee of Geohazard Preventions in China.